VOLUME 77 SEPARATE No. 86

Rochester Public Library
115 South Avenue
ROCHESTER 4, N. Y.

PROCEEDINGS

AMERICAN SOCIETY OF CIVIL ENGINEERS

AUGUST, 1951

GROUND-WATER MOVEMENT CONTROLLED THROUGH SPREADING

By Paul Baumann, M. ASCE

IRRIGATION DIVISION

Copyright 1951 by the AMERICAN SOCIETY OF CIVIL ENGINEERS
Printed in the United States of America

Headquarters of the Society
33 W. 39th St.
New York 18, N.Y.

PRICE $0.50 PER COPY

r620.L

The Society is not responsible for any statement made or opinion expressed in its publications

---

HINTS TO AUTHORS

Those who are planning papers for submission to PROCEEDINGS-SEPARATES *will expedite action measurably by first studying the standard instructions as to style, content, and format. For reprints, address the Manager, Technical Publications, 33 W. 39th St., New York 18, N. Y.*

Published at Prince and Lemon Streets, Lancaster, Pa., by the American Society of Civil Engineers. Editorial and General Offices at 33 West Thirty-ninth Street, New York 18, N. Y. Reprints from this publication may be made on condition that the full title of paper, name of author, page reference, and date of publication by the Society are given.

Proceedings—Vol. 77 August, 1951 Separate No. 86

AMERICAN SOCIETY OF CIVIL ENGINEERS

Founded November 5, 1852

PAPERS

GROUND-WATER MOVEMENT CONTROLLED THROUGH SPREADING

By Paul Baumann,[1] M. ASCE

Synopsis

Over a period of years the Los Angeles County Flood Control District in California, under the writer's direction, has been engaged in water conservation by the diversion of clear stream flow to off-channel areas, causing the water to percolate into the soil from shallow basins and thereby adding it to the ground-water supply. This operation is known as spreading, and the areas upon which it is performed are called spreading grounds.[2]

In the course of spreading a mound will be formed above the initial ground-water table. The mound will be two dimensional or three dimensional, depending on the shape of the spreading ground. The recharge of ground water through wells is a special, three-dimensional case. The control of sea water intrusion into ground-water basins is of particular significance. The configuration of the mound, its limiting magnitude, its effective, temporary water retention both as to volume and time, its flow net for potential flow, and the drainage of the water stored in the mound are analyzed in this paper.

Finally, the theoretical results are compared with results derived from model tests on two-dimensional flow.

Introduction

The mound is two dimensional if spreading is done from strip areas and three dimensional if the area approximates a circle. The height H to which a mound may rise during a spreading operation depends on: (1) Rate (q_o) of spreading—that is, the rate of infiltration; (2) duration (T) of spreading; (3) permeability (K) of the soil; (4) porosity (μ) of the soil; (5) vertical distance (D) between the initial ground-water surface and the ground surface;

Note.—Written comments are invited for publication; the last discussion should be submitted by February 1, 1952.

[1] Asst. Chf. Engr., Los Angeles County Flood Control Dist., Los Angeles, Calif.

[2] "Correlating Flood Control and Water Supply, Los Angeles Coastal Plain," by Finley B. Laverty, *Transactions*, ASCE, Vol. 111, 1946, p. 1127.

(6) depth (a_o) between initial ground-water surface and impervious stratum; (7) slope (i) of the impervious stratum; and (8) horizontal distance (L_d) to a control through which the downstream boundary conditions are uniquely established.

The mound phenomenon must be divided into four distinct phases. The first three occur during its growth and the fourth phase during its disappearance after discontinuation of spreading.

The First Phase.—The first phase consists of a mound wave created when the inflowing water is being put into storage, necessarily above the initial ground-water surface. For constant inflow q_o this wave must grow in magnitude and thereby represents a case of unsteady flow. The growth of this wave continues until a boundary is reached. The boundary in regard to x is called the "lateral control," as represented by a river, a lake, or a trench. The boundary in regard to y is called the "potential control." It is the surface of the spreading basin.

The Second Phase.—The second phase is transitory. It begins when: (a) The wave front reaches the lateral control, or (b) the wave crest reaches the potential control. In case (a), the wave length L has reached its maximum value. Discharge now begins and increases until it is equal to the inflow q_o. In case (b), the height H of the wave remains constant while the length L increases and, in the absence of a lateral control, theoretically becomes infinite. Hence, all the flow is put into storage at a steadily decreasing rate.

The Third Phase.—In the presence of a lateral control, stationary flow will occur during the third phase. Under these conditions potential flow will develop, and the storage in the mound will reach its maximum for a constant inflow q_o. It may greatly exceed available surface storage.

The Fourth Phase.—If the mound has reached equilibrium in the presence of a lateral control and if spreading is discontinued suddenly, it will drain itself in the course of time. If the mound has reached the potential control in the absence of a lateral control, and if spreading has subsequently been continued until, theoretically, the inflow q_o has become zero and the wave length L has become infinity, then this mound will never drain itself as long as there is no extraction from it. This serves to emphasize the fact that the drainage phenomenon is primarily related to the existence of a lateral control.

General Conditions.—The mathematical analysis of the mound phenomenon is based on the Darcy law[3,4] of percolation of water through sand. This law is valid as long as the flow is laminar. Laminar flow is governed by the Reynolds[5,6] number **R**. M. Muskat[7] and others have found that, for sand, laminar flow takes place if $R \leqq 1$.

Furthermore, the idealized soil is assumed to be homogeneous as well as isotropic. Hence, the permeability remains constant irrespective of the direc-

[3] "Les fontaines publiques de la ville de Dijon," by Henri Darcy, Dalmont, Paris, 1856.
[4] "Recherches physica-mathematiques sur la théorie du mouvement des eaux courantes," by G. C. F. M. R. de Prony, Mémoires de l'Institute National, Paris, 1804.
[5] "Papers on Mechanical and Physical Subjects," by Osborne Reynolds, C. J. Clay and Sons, Cambridge, England, 1903.
[6] "The Two Manners of Motion of Water," by Osborne Reynolds, *Proceedings*, Royal Institution of Great Britain, Vol. XI, 1884–1886, p. 44.
[7] "The Flow of Homogeneous Fluids Through Porous Media," by M. Muskat, McGraw-Hill Book Co., Inc., New York, N. Y., 1st Ed., 1937.

tion of flow which, admittedly, is not in keeping with natural soils. However, spreading grounds are located in soils that approach idealized conditions extending over great distances. Within these distances permeability and porosity of the soil and slope of the impervious stratum may be expressed by average values with satisfactory results.

Generally, the storage in the part of the mound directly beneath the spreading ground is small as compared to the total storage. Therefore, it may be neglected except in special cases.

The slope (i) of the impervious stratum is generally small, namely, of the order $\leqq 0.01$.

PART I.—THE TWO-DIMENSIONAL FLOW OF WATER THROUGH GRANULAR SOIL

1.—Analysis of Unsteady Ground-Water Flow

Outstanding among the classical presentations on unsteady ground-water flow is the one due to M. J. Boussinesq.[8] He derived the differential equation—

$$\frac{\partial y}{\partial t} = \frac{K}{\mu}\left[y\frac{\partial^2 y}{\partial x^2} + \left(\frac{\partial y}{\partial x}\right)^2 - i\frac{\partial y}{\partial x}\right] \quad \ldots\ldots\ldots\ldots\ldots (1)$$

—which expresses this phenomenon and in which x and y are the coordinates of the free water surface. If the flow becomes steady or stationary, Eq. 1 reduces to

$$q_o = K\,y\left(i - \frac{\partial y}{\partial x}\right) \quad \ldots\ldots\ldots\ldots\ldots\ldots\ldots (2)$$

which is known as the Dupuit[9] equation or theorem. The validity of Eq. 2 requires that the vertical components of the velocity vectors are small as compared to the horizontal ones. Where such is the case, calculations based on the Dupuit equation lead to satisfactory solutions.

Eq. 1 is not integrable by exact calculus methods. Considering the fact that, normally in ground-water flow, the slope of the water surface and the height of the mound relative to the initial ground-water depth a_o are small, Boussinesq proceeds in neglecting $\left(\frac{\partial y}{\partial x}\right)^2$ and in making $y = a_o$. Hence, Eq. 1 reduces to

$$\frac{\partial y}{\partial t} = \frac{K}{\mu}\left(a_o\frac{\partial^2 y}{\partial x^2} - i\frac{\partial y}{\partial x}\right) \quad \ldots\ldots\ldots\ldots\ldots\ldots (3)$$

Considering the further fact, however, that in connection with ground-water phenomena related to spreading, the term $i\frac{\partial y}{\partial x}$ is normally of the same order of magnitude as $\left(\frac{\partial y}{\partial x}\right)^2$ if, indeed, it is not generally smaller; $i\frac{\partial y}{\partial x}$ appears

[8] "Essai sur la Théorie des Eaux Courantes," by M. J. Boussinesq, Memoires à l'Académie des Sciences de l'Institut de France, Vol. 23, 1877, p. 257.

[9] "Etudes théoriques et pratiques sur le mouvement des eaux Courantes," by Jules Dupuit Carilian-Goeury, Paris, 1948.

negligible with equal justification. Actually these terms are of opposite sign so long as i and $\frac{\partial y}{\partial x}$ are of equal sign. Their difference, then, is of higher order of smallness. Hence the neglect of both terms is, probably, a closer approximation than the neglect of $\left(\frac{\partial y}{\partial x}\right)^2$ only. The exception to this rule and its significance will be referred to in its proper place. With this neglect, or for $i = 0$, in Eq. 3 there results

$$\frac{\partial y}{\partial t} = K \frac{a_o}{\mu} \frac{\partial^2 y}{\partial x^2} \quad \ldots\ldots\ldots\ldots\ldots\ldots\ldots\ldots\ldots\ldots (4)$$

which is identical in form with the well-known differential equation for the flow of heat through a nonradiating prismatic bar. Boussinesq referred to this analogue three quarters of a century ago.

Heat Analogue Solution; Bar of Finite Length[10] *(First, Second, and Fourth Phase).*—Based on the analogue of the flow of heat through a prismatic, nonradiating bar of length L_d with a continuous and constant heat source at the origin $x = 0$ (spreading ground) and constant temperature at the opposite end $x = L_d$ (control), the following solution for the first, second, and fourth phase of the mound phenomenon was developed for $i \neq 0$.

The Growing Mound Between the Spreading Ground and the Control.—To simplify typography, let:

$$j = \frac{K a_o t}{\mu} \quad \ldots\ldots\ldots\ldots\ldots\ldots\ldots\ldots\ldots\ldots (5)$$

It may be verified through differentiation that

$$y = C_1 e^{-\beta^2 j} \cos \beta x + C_2 x + C_3 \quad \ldots\ldots\ldots\ldots\ldots\ldots (6)$$

is a particular solution of Eq. 4 in which C_1, C_2, C_3, and β are arbitrary constants. It does not satisfy the boundary conditions for the growing mound phenomenon, however. These conditions are

1. $y = 0$ at $t = 0$ for all values of x;
2. $y = 0$ at $x = L_d$ for all values of t in which $0 < L_d < \infty$; and
3. $y = f(x)$ at $t = \infty$.

Based on the fundamental concept that $y \ll a_o$ upon which Eq. 4 is predicated, the linear equation for $f(x)$

$$y = \left(\frac{q}{K a_o} - i\right)(L_d - x) \quad \ldots\ldots\ldots\ldots\ldots\ldots\ldots (7)$$

is the approximate equation for the stable mound at $t = \infty$. The relations—

$$\beta = \frac{(2n - 1)\pi}{2 L_d} \quad \ldots\ldots\ldots\ldots\ldots\ldots\ldots\ldots (8a)$$

[10] "Conduction of Heat in Solids," by H. S. Carslaw and J. C. Yaeger, Oxford University Press, Oxford, England, 1947.

and

$$C_2 L_d = -C_3 \quad \ldots\ldots\ldots\ldots\ldots\ldots\ldots\ldots (8b)$$

—satisfy condition 2; and

$$C_2 = -\left(\frac{q}{K a_o} - 1\right) \quad \ldots\ldots\ldots\ldots\ldots\ldots\ldots\ldots (8c)$$

satisfies condition 3. Hence Eq. 6 becomes:

$$y = C_1 e^{-\beta^2 i} \cos \frac{(2n-1)\pi}{2 L_d} x + \left(\frac{q}{K a_o} - i\right)(L_d - x) \quad \ldots\ldots\ldots (9)$$

Eq. 9 still does not satisfy condition 1, however.

A Fourier series expansion for the equation of the stable mound is

$$y = \left(\frac{q}{K a_o} - i\right)(L_d - x) = \frac{8\left(\frac{q}{K a_o} - i\right) L_d}{\pi^2} \sum_{n=1}^{n=\infty} \frac{1}{(2n-1)^2} \times \cos \frac{(2n-1)\pi x}{2 L_d} \quad \ldots\ldots (10a)$$

and the final equation then becomes

$$y = \left(\frac{q}{K a_o} - i\right)(L_d - x) - \frac{8\left(\frac{q}{K a_o} - i\right) L_d}{\pi^2} \sum_{n=1}^{n=\infty} \frac{1}{(2n-1)^2} \times \left(\cos \frac{(2n-1)\pi x}{2 L_d}\right) e^{-\beta^2 i} \quad \ldots\ldots (10b)$$

which satisfies all of the boundary conditions.

The Disappearing Mound Between the Spreading Ground and the Control.—The boundary conditions now become:

(*a*) $y = \left(\frac{q}{K a_o} - i\right)(L_d - x)$ at $t = 0$;
(*b*) $y = 0$ at $x = L_d$ for all values of t; and
(*c*) $y = 0$ at $t = \infty$ for all values of x.

Eq. 10*b* indicates that condition (*a*) is satisfied if:

$$y = \frac{8(q - K a_o i) L_d}{K a_o \pi^2} \sum_{n=1}^{n=\infty} \frac{1}{(2n-1)^2} \left(\cos \frac{(2n-1)\pi x}{2 L_d}\right) e^{-\beta^2 i} \quad \ldots (11)$$

and that conditions (*b*) and (*c*) are likewise satisfied.

The General Case of the Unsteady Mound for $i \neq 0$.—The foregoing was predicated on the presence of discontinuity immediately upstream from the spreading ground, for example, in the form of a basin barrier. In the absence of such a discontinuity the growth of the mound downstream from the spreading ground gives rise to a backwater condition upstream from it. Hence, there

are three distinct zones to be considered as indicated in Fig. 1. The true configuration of the stable mound will be analyzed in a subsequent section. In the following, the mound surface in zone II is considered parallel to, and the distance H_d above, the initial ground-water surface. For a constant ground-water flow $q = K\,a_o\,i$:

$$K\,a_o\,i = K\,(a_o + y)\left(i - \frac{d\,(a_o + y)}{dx}\right) \ldots\ldots\ldots\ldots (12a)$$

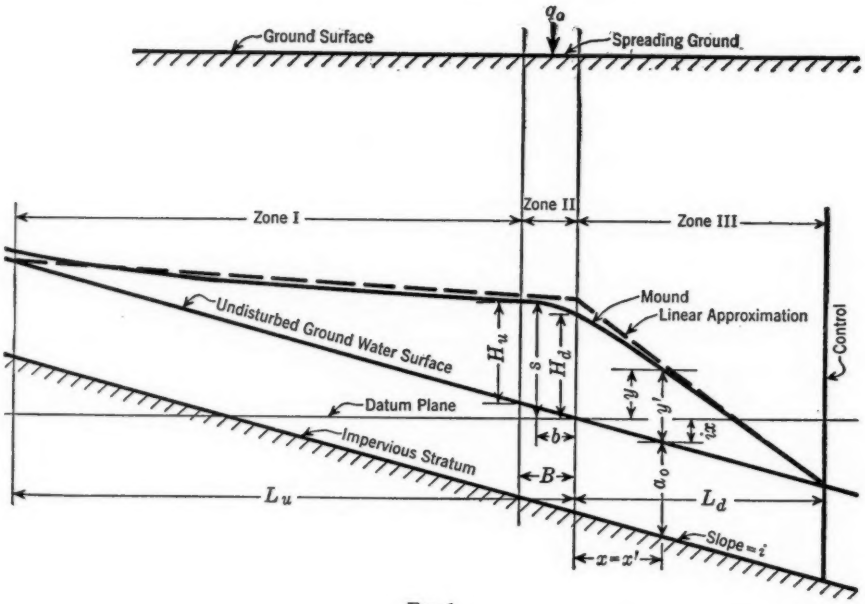

FIG. 1

Upon integration, Eq. 12a results in:

$$-\,i\,(x - B) = (H_d - y) - a_o \log_e \frac{y}{H_d} \ldots\ldots\ldots\ldots (12b)$$

in which B = width of spreading ground. Since $2 > \frac{y}{H_d} > 0$:

$$\log_e \frac{y}{H_d} = \frac{y - H_d}{H_d} - \frac{1}{2}\left(\frac{y - H_d}{H_d}\right)^2 + \frac{1}{3}\left(\frac{y - H_d}{H_d}\right)^3 \ldots\ldots\ldots (13)$$

After neglecting B and all but the first term, an approximate, linear equation is:

$$y = \frac{H\,i}{a_o + H}\,(L_u + x) \ldots\ldots\ldots\ldots\ldots\ldots (14)$$

in which $0 < i < 0.01$.

The stable mound will now be considered approximated by Eqs. 7 and 14, as indicated by dash lines in Fig. 1. A Fourier series, to describe this stable mound in one equation, with the origin at the spreading ground, is

$$y = \left(\frac{L}{\pi}\right)^2 \frac{H}{L_u\,L_d} \sum_{n=1}^{n=\infty} \frac{\cos\dfrac{n\,\pi\,x}{L} - (-1)^n \cos\dfrac{n\,\pi\,(x + L_u - L_d)}{L}}{n^2} \ldots (15)$$

in which $-L_u < x < L_d$ and $L_u + L_d = L$. An equation which satisfies Eq. 4 can be written for the disappearing mound.

$$y = \left(\frac{L}{\pi}\right)^2 \frac{H}{L_u L_d} \times \sum_{n=1}^{n=\infty} \left[\frac{\cos \frac{n\pi x}{L} - (-1)^n \cos \frac{n\pi (x + L_u - L_d)}{L}}{n^2} \right] e^{-(n\pi/L)^2 i} \quad . . (16)$$

For the growing mound two equations are necessary, for zone III—

$$y = H - \frac{q_o x}{K a_o} - \frac{L^2 H}{\pi^2 L_u L_d} \times \sum_{n=1}^{n=\infty} \left[\frac{\cos \frac{n\pi x}{L} - (-1)^n \cos \frac{n\pi (x + L_u - L_d)}{L}}{n^2} \right] e^{-(n\pi/L)^2 i} \quad . . (17a)$$

and for zone I—

$$y = \frac{H}{L_u}(L_u + x) - \frac{L^2 H}{\pi^2 L_u L_d} \times \sum_{n=1}^{n=\infty} \left[\frac{\cos \frac{n\pi x}{L} - (-1)^n \cos \frac{n\pi (x + L_u - L_d)}{L}}{n^2} \right] e^{-(n\pi/L)^2 i} \quad . . (17b)$$

It can be verified easily that Eq. 17 has the same value at $x = 0$.

Eqs. 16 and 17, with the previous equations defining L_d, L_u, and H, constitute a general solution of the shape of the unsteady mound within the limits of the initial assumptions and approximations made. Fig. 2 shows the configurations at various times t for the growing (dash lines) and the disappearing (solid lines) mound for the following numerical values: $L_d = 4$ ft; $q_o = 0.82$ cu ft per hr; $K = 25$ ft per hr; $a_o = 0.5$ ft; and $\mu = 0.15$ for a growing mound (dash line in Fig. 2) and 0.06 for a draining mound (solid line in Fig. 2). These values correspond to those in the comprehensive model tests, except that $i \neq 0$. It is interesting to note a division of flow from the spreading ground between zones I and III during part of the growth. This conforms to the requirement of synchronous growth of the two zones at $x = 0$. The initial ground-water flow is checked during this period and goes entirely into storage in zone I. This feature is of particular significance in the control of sea water intrusion. It shows that the latter is checked when the infiltrated fresh water reaches the saline ground-water table. To maintain control indefinitely the rate of infiltration must be such as to cause rise of the mound to at least mean sea level. The use of recharge wells for this purpose will be discussed in the chapter on three-dimensional flow.

Eq. 4, which forms the basis for this solution, holds true strictly for $i = 0$ only, although it should lead to satisfactory results for $i \neq 0$ so long as $\left(\frac{\partial y}{\partial x}\right)^2$ and $i \frac{\partial y}{\partial x}$ are small, of the same order of magnitude and opposite in sign. The latter condition is not satisfied during just the aforementioned

initial period of infiltrated flow into zone 1. However, the influence on the mound configuration of this discrepancy is not important in the light of the mathematical simplification thus achieved. Hence, mathematically, the base of the triangular mound is horizontal. This gives rise to a fictitious outflow

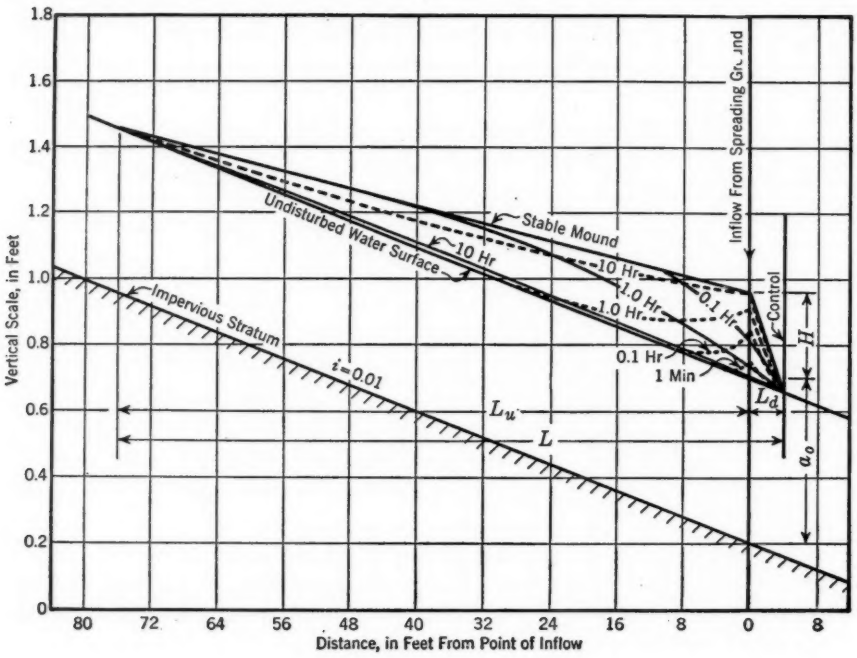

FIG. 2

at the upstream end and a discontinuity in slope because of the approximation of the upstream curve by a straight line. To conform to the physical system, the mathematical system must be superposed on the sloping base. The accumulated sum of the mathematical outflows at the two ends corresponds to the effective pore volume in the triangular mound, drained during time t.

The flow at any section is:

$$q = K\,a_o\left(i - \frac{\partial y}{\partial x}\right) - K\,a_o i = -K\,a_o\frac{\partial y}{\partial x} \quad \ldots\ldots\ldots\ldots (18)$$

Hence, the outflow at the control during the disappearance is

$$q_d = \frac{2\,K\,a_o\,L\,H}{\pi\,L_u\,L_d}\sum_{n=1}^{n=\infty}\frac{\left(\sin\frac{n\,\pi\,L_d}{L}\right)(1-(-1)^n)}{n}\,e^{-(n\,\pi/L^2)\,j} \quad \ldots\ldots (19a)$$

and during the growth

$$q_g = q_o - \frac{K\,a_o\,L\,H}{\pi\,L_u\,L_d}\sum_{n=1}^{n=\infty}\left[\frac{2\sin\frac{n\,\pi\,L_d}{L}}{n}\right]e^{-(n\,\pi/L)^2 j} \quad \ldots\ldots\ldots (19b)$$

For $L_u = L_d$ Eqs. 16, 17, and 19 express the conditions for the symmetrical mound ($i = 0$).

2.—The True Configuration of the Stable Mound for $i \neq 0$

Based on the coordinate system shown in Fig. 1, for zone III:

$$K a_o i + q_o = - K (y + a_o + i x) \frac{dy}{dx} \quad \ldots\ldots (20)$$

After rotating the x-axis so as to be parallel to i

$$x' = x \quad \ldots\ldots (21a)$$

and

$$y' = y + i x \quad \ldots\ldots (21b)$$

The quantity $i y$ is neglected in Eq. 21a. After introducing Eqs. 21 into Eq. 20 and integrating:

$$(y')^2 + 2 a_o y' + \frac{2 q_o}{K} x' = 2 i \int y' dx' + C \quad \ldots\ldots (22)$$

It is approximately true that

$$\int y' dx' = \frac{H_d + y'}{2} x' \quad \ldots\ldots (23)$$

Also when $x' = 0$:

$$y' = H_d \quad \ldots\ldots (24a)$$

and

$$C = H^2_d + 2 a_o H_d \quad \ldots\ldots (24b)$$

Substituting Eqs. 23 and 24 in Eq. 22 and solving for y':

$$y' = - \left(\frac{2 a_o - i x'}{2} \right) + \sqrt{\left(\frac{2 a_o - i x'}{2} \right)^2 - \left[\frac{2 q_o x'}{K} - ((H_d + a_o)^2 - a^2_o) - i x' H_o \right]} \quad \ldots\ldots (25)$$

For $x' = L'$, $y' = 0$. Hence:

$$H_d = - \left(\frac{2 a_o + i L'}{2} \right) + \sqrt{\left(\frac{2 a_o + i L'}{2} \right)^2 + \frac{2 q_o L'}{K}} \quad \ldots\ldots (26)$$

For zone II:

$$K a_o i + \frac{q_o}{B} (B + b) = - K (s + a_o + i b) \frac{ds}{db} \quad \ldots\ldots (27)$$

Hence

$$\frac{ds}{db} = - \left[\frac{\frac{q_o b}{B K} + \frac{q_o}{K} + a_o i}{i b + s + a_o} \right] \quad \ldots\ldots (28)$$

which is a linear, fractional, nonhomogeneous, differential equation. Substituting $s = s_1 + M$ and $b = b_1 + N$ in Eq. 28 and solving for M and N result in the homogeneous equation:

$$\frac{ds_1}{db_1} = -\frac{q_o\, b_1}{B\, K\, (i\, b_1 + s_1)} \quad \ldots\ldots\ldots\ldots\ldots\ldots\ldots\ldots (29)$$

Introducing $U = \frac{b_1}{s_1}$ and $db_1 = s_1\, dU + U\, ds_1$; integrating and neglecting i^2 and i in $\frac{2\, q_o\, b_1}{B\, K\, s_1} + i$:

$$0 = \log_e \left[\frac{\frac{q_o\, b^2_1}{B\, K} + i\, b_1\, s_1 + s^2_1}{C^2} \right] - \frac{i}{\sqrt{\frac{q_o}{B\, K}}} \tan^{-1} \frac{\sqrt{\frac{q_o}{B\, K}}}{s_1} b_1 \ldots\ldots (30)$$

in which, with close approximation:

$$C^2 = \frac{B \left(\frac{q_o}{K} + 2\, a_o\, i \right) + \left((H_d + a_o) - \frac{B\, i}{2} \right)^2}{e^u} \quad \ldots\ldots\ldots\ldots (31)$$

in which (to simplify typography):

$$u = \frac{i}{\sqrt{\frac{q_o}{B\, K}}} \tan^{-1} \frac{\sqrt{\frac{q_o\, B}{K}} \left(1 + \frac{K\, a_o\, i}{q_o} \right)}{(H_d + a_o) - i\, B}$$

The backup curve in zone I is determined by Eq. 12*b*. Hence the configuration of the stable mound for $i \neq 0$ is a steady curve, expressed by Eqs. 25, 30, and 12 and shown in Fig. 1.

3.—Approximate Equations For Unsteady Ground-Water Flow

The Unique Flow Function—First Phase (Zone III).—In view of the limitations imposed upon Eq. 3, it is axiomatic that the respective solutions are valid only within these limitations, namely, $y \ll a_o$ and $\frac{dy}{dx}$ and i is very small. Although the latter condition is reasonably satisfied in connection with these phenomena, the former quite often is not. Hence, it was desirable to find a unique function $q = f(x)$ for unsteady flow which is in close agreement with those based on Eq. 3 within the imposed limitations but which permits extrapolation beyond these limits. This function must satisfy the following conditions:

1. $q = q'$ at $x = 0$, in which q' is that portion of q_o, flowing into zone III;
2. $q = 0$ at $x = L$;
3. $\frac{dy}{dx} = 0$ at $x = L$; and
4. q must fade away as $x \rightarrow L$.

The first three conditions are satisfied by a multitude of functions, whereas an exponential function is required to satisfy condition 4. All four conditions are satisfied by:

$$q = q' \left(1 - \frac{e\,x}{L}\, e^{-x/L}\right) \ldots\ldots\ldots\ldots\ldots\ldots\ldots (32)$$

In accordance with Fig. 3:

$$K\,a_o\,i + q = -\,(y + a_o + i\,x)\,K\,\frac{dy}{dx} \ldots\ldots\ldots\ldots\ldots (33)$$

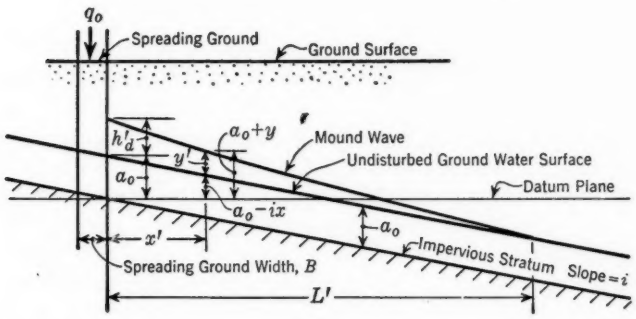

FIG. 3

After rotating the axes so as to make the x-axis parallel to i:

$$x' = x \ldots\ldots\ldots\ldots\ldots\ldots\ldots\ldots (34a)$$

since $i\,y$ may be neglected again and

$$y' = y + i\,x \ldots\ldots\ldots\ldots\ldots\ldots\ldots (34b)$$

Hence:

$$\frac{dy}{dx} = \frac{dy'}{dx'} - i \ldots\ldots\ldots\ldots\ldots\ldots\ldots (35)$$

and

$$\frac{q}{K}\,dx' = -\,(y' + a_o)\,dy' + y'\,i\,dx' \ldots\ldots\ldots\ldots\ldots (36)$$

Substituting for q and integrating

$$\frac{q'}{K}\,(x' + (x' + L')\,e^{(L'-x')/L'}) + \frac{(y')^2}{2} + y'\,a_o - i\int_o^{x'} y'\,dx' = C \ldots (37)$$

The last member on the left side (which represents a small fraction of the area of the mound wave) may be simplified; thus

$$\int_o^{x'} y'\,dx' = \left(\frac{h'_d + y'}{2}\right) x' \ldots\ldots\ldots\ldots\ldots (38)$$

and

$$(y')^2 + 2\,a_o\,y' + \frac{2\,q'}{K}\,(x' + (x' + L')\,e^{(L'-x')/L'}) - i\,x'\,(h'_d + y') = C \ldots (39)$$

For $x' = 0$, $y' = h'_d$ and $C = h'^2_d + 2\,a_o\,h'_d + \frac{2\,q'}{K}\,L'\,e$; therefore:

$$y' = -\left(\frac{2\,a_o - i\,x'}{2}\right) + \sqrt{\left(\frac{2\,a_o - i\,x'}{2}\right)^2 - \left\{\frac{2\,q'}{K}\left[x' + e\,L'\left(\left(\frac{x'}{L'} + 1\right)e^{-x'/L'} - 1\right)\right] - ((h'_d + a_o)^2 - a_o^2) - i\,x'\,h'_d\right\}} \ldots (40)$$

For $x' = L'$, $y' = 0$, and

$$h'_d = -\left(\frac{2\,a_o + i\,L'}{2}\right) + \sqrt{\left(\frac{2\,a_o + i\,L'}{2}\right)^2 + \frac{2\,q'\,L'}{K}\,(1 + (2 - e))} \ldots . (41)$$

The quantity q' flows into zone III. The remainder of q_o flows into storage in zones II and I. Except for a short initial period, the storage in zone II may be neglected. Hence q' follows from the condition of synchronized rise at $x' = 0$. For $i = 0$, and neglecting zone II, $q' = q_o$.

The Unique Time Function—Second Phase.—

Case (a).—At the instant the mound wave reaches the lateral control at $x' = L'$, the discharge there is zero, and the configuration of the wave is expressed by Eq. 40. On the other hand the configuration of the stable mound is expressed by Eq. 25. If the approximate time T_2 of the transition is to be finite (for example, the time during which 95% of the transition takes place) then within this period the term $e\,L'\left(\left(\frac{x'}{L'} + 1\right)e^{-x'/L'} - 1\right)$ in Eq. 40 must fade away; h'_d must change to H_d (which is accomplished if $(2 - e)$ in Eq. 41 fades away); and q' must change to q_o. Furthermore, at any time t the total inflow must equal the total storage plus the total outflow.

The unique time function that satisfies these conditions is:

$$f(t) = 1 - \frac{e\,t}{T_2}\,e^{-t/T_2} \ldots \ldots \ldots \ldots \ldots \ldots (42)$$

and the mound equation for the second phase is

$$y' = -\left(\frac{2\,a_o - i\,x'}{2}\right) + \sqrt{\left(\frac{2\,a_o - i\,x'}{2}\right)^2 - \left\{\frac{2\,x'}{K}\left[q_o + q'\left[\left(1 + \frac{1}{x'}\right)\left(e\,L'\left(\frac{x'}{L'} + 1\right)e^{-x'/L'} - 1\right) - q_o\right]\left(1 - \frac{e\,t}{T_2}e^{-t/T_2}\right)\right] - \left((h'_d - a_o)^2 - a_o^2\right) - i\,x'\,h'_d\right\}} \ldots (43)$$

in which:

$$h'_d = -\left(\frac{2\,a_o - i\,L'}{2}\right) + \sqrt{\left(\frac{2\,a_o - i\,L'}{2}\right)^2 + \frac{2\,L'}{K}\left[q_o + \left(q'\,(3 - e) - q_o\right)\left(1 - \frac{e\,t}{T_2}e^{-t/T_2}\right)\right]} \ldots (44)$$

Case (b).—If the mound wave rises to the potential control in the absence of a lateral control, then from Eq. 41, it becomes evident that for the wave height h'_d to remain constant, the product $q'\,L' = q_o\,L'$ must remain constant. Hence, as the wave continues to grow in length, the inflow q_o must diminish proportionally. This is strictly true for $i = 0$ and nearly so for $i\,L' \ll 2\,a_o$.

From a practical point of view this significance of the wave reaching the surface is that "waterlogging" of the ground may become critical, not only upstream from the spreading ground but also downstream from it.

The Approximate Time Requirement.—

First Phase.—Since the initial ground-water flow ($K\,a_o\,i$) remains unchanged throughout the wave configuration, it is evident that the water stored in zone III must be caused entirely by the flow q' and that, in order to satisfy continuity:

$$V'_1 = \mu \int_o^{L'} y'\,dx' = \int_o^{T'_1} q'\,dt \ldots\ldots\ldots\ldots\ldots\ldots (45)$$

in which: V'_1 = pore volume; and T'_1 = time required to create wave length L' and height h'. The exact integration of Eq. 45 would be a formidable task so long as i is a factor in Eq. 40 and q' is variable. A graphical solution would be called for whereby the relation between t, q', h', and L', for arbitrary slopes i, could be established with close approximation.

Actually the influence on the final result of $0 < i < 0.01$ is such that it does not differ significantly from that due to $i = 0$.

For $i = 0$ Eq. 40 reduces to:

$$y = -a_o + \sqrt{(h + a_o)^2 - \frac{2\,q_o}{K}\left[x + e\,L\left(\left(\frac{x}{L} + 1\right)e^{-x/L} - 1\right)\right]} \ldots (46)$$

and Eq. 41 to

$$h = -a_o + \sqrt{a_o^2 + \frac{2\,q_o\,L}{K}(3 - e)} \ldots\ldots\ldots\ldots\ldots (47)$$

The determination of the pore volume of the mound wave as represented by Eq. 46 is facilitated by expanding it into a binomial which converges for all values $x < L$, $(h + a_o) > \frac{2\,q_o}{K}\left[x + e\,L\left(\left(\frac{x}{L} + 1\right)e^{-x/L} - 1\right)\right]$. Hence,

$$y = h - \frac{q_o}{K\,(a_o + h)}\left[x + eL\left(\left(\frac{x}{L} + 1\right)e^{-x/L} - 1\right)\right] \ldots\ldots (48)$$

For $y = 0$ and $x = L$, from Eq. 48:

$$h^2 + a_o\,h = \frac{q_o\,L}{K}(3 - e) \ldots\ldots\ldots\ldots\ldots\ldots (49a)$$

whereas, from Eq. 47:

$$h^2 + 2\,a_o\,h = \frac{2\,q_o\,L}{K}(3 - e) \ldots\ldots\ldots\ldots\ldots\ldots (49b)$$

It is obvious that, for $a_o = 0$, h^2 from Eq. 47 is just twice that from Eq. 48. Therefore Eq. 47 is closely approximated by

$$h = \frac{\check{c}\,q_o\,L}{K\,(a_o + h)}(3 - e) \ldots\ldots\ldots\ldots\ldots\ldots (50)$$

if the values shown in Fig. 4 are used for $\bar{c}$. This coefficient is not applicable to Eq. 48 if $x \neq L$, because $\bar{c}$ would have to be a function of x for $a_o \leqq h$. However, for $a_o > h$, Eq. 48 is a satisfactory approximation if $\bar{c} = 1$. The

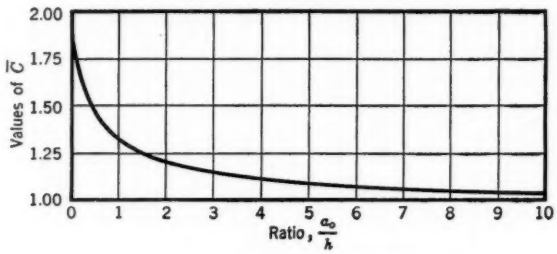

FIG. 4

volume V_1, based on Eq. 48 and $a_o > h$, is:

$$V_1 = \mu \int_o^L y\,dx = \mu \int_o^L \times\left\{h - \frac{q_o}{K\,(h + a_o)}\left[x + e\,L\left(\left(\frac{x}{L} + 1\right)e^{-x/L} - 1\right)\right]\right\} dx = q_o\,T_1 \ldots (51)$$

and upon integration

$$T_1 = \mu\left[\frac{L\,h}{q_o} - \frac{L^2}{K\,(h + a_o)}\left(e - \frac{5}{2}\right)\right] \ldots\ldots\ldots\ldots (52)$$

The Second Phase, Case (a).—The binomial expansion of Eq. 43 for $a_o > h$ and $i = 0$

$$y = h - \frac{q_o}{K\,(h + a_o)}\left[x + e\,L\left(\left(\frac{x}{L} + 1\right)e^{-x/L} - 1\right)\left(1 - \frac{e\,t}{T_2}e^{-t/T_2}\right)\right] \ldots (53)$$

The outflow q at $x = L$ at any time, t, is:

$$q = -\,K\,a_o\left(\frac{dy}{dx}\right)_L \ldots\ldots\ldots\ldots\ldots\ldots (54)$$

and the volume ΔV_d of water discharged during t is:

$$\Delta V_d = \int_o^t q\,dt - K\,a_o \int_o^t \left(\frac{dy}{dx}\right)_L dt \ldots\ldots\ldots\ldots (55)$$

Since t is not affected in regard to x

$$\left(\frac{dy}{dx}\right)_L = -\,\frac{\bar{c}\,q_o}{K\,(h + a_o)}\left(\frac{e\,t}{T_2}e^{-t/T_2}\right) \ldots\ldots\ldots\ldots (56)$$

and from Eq. 55

$$\Delta V_d = +\,\frac{\bar{c}_m\,q_o\,a_o\,e}{(h_m + a_o)}\int_o^t \frac{t}{T_2}e^{-t/T_2}\,dt \ldots\ldots\ldots\ldots (57)$$

in which $h_m = \frac{h + H}{2}$ is constant in order to make integration possible, and $\bar{c}_m$ is determined from Fig. 4 for $\frac{a_o}{h_m}$. The use of this mean value is permissible since the ratio h/H varies between the order of 1/2 and 1/3 for $a_o = 0$ and for a very large value of a_o; and $\bar{c}$ also applies to the binomial of Eq. 25 for $i = 0$ and $x = L$. For normal values of a_o the ratio h/H is nearly constant—namely 1/3; and $h_m \sim 2/3\ H$. Integrating Eq. 57:

$$\Delta V_d = - \frac{\bar{c}_m\, q_o\, a_o\, e}{(h_m + a_o)} \left[(T_2 + t)\, e^{-t/T_2} - T_2\right] \ldots\ldots\ldots\ldots (58)$$

and the approximate, total accumulated outflow during the time T_2

$$V_d = \frac{\bar{c}_m\, q_o\, a_o\, T_2}{(h_m + a_o)} (e - 2) \ldots\ldots\ldots\ldots\ldots\ldots (59)$$

The volume V_m of water stored in the mound during the time T_2 is

$$V_m = \mu \int_o^L \Delta y\, dx \ldots\ldots\ldots\ldots\ldots\ldots (60)$$

in which Δy is the difference between y from Eq. 25 and from Eq. 43 for $i = 0$. Using the binomial of both equations:

$$V_m = \mu \left[(H - h)\, L + \frac{q_o\, L^2}{K\,(h + a_o)} \left(\frac{H - h}{2\,(H + a_o)}\right) - (3 - e)\right] \ldots (61)$$

Because of continuity

$$q_o\, T_2 - \Delta V_d = V_m \ldots\ldots\ldots\ldots\ldots\ldots (62)$$

and

$$T_2 = \frac{\mu}{1 - \frac{\bar{c}_m\,(e - 2)}{h_m + a_o}} \left[\frac{(H - h)\, L}{q_o} + \frac{L^2}{K\,(h + a_o)} \left(\frac{H - h}{2\,(H + a_o)} - (3 - e)\right)\right] \ldots (63)$$

The Unique Time Function—Fourth Phase.—The mathematical analysis, based on Eq. 4, of the drainage of the mound upon sudden discontinuation of spreading after it had reached a stationary condition has been treated in Sect. 1 for the general case, $i \neq 0$. The following approximate solution leads to results which are a fair representation of the drainage phenomenon for $i = 0$.

During the drainage period the flow through the downstream control is

$$q = - K\, a_o \left(\frac{dy}{dx}\right)_L \ldots\ldots\ldots\ldots\ldots\ldots (64)$$

in which $\left(\frac{dy}{dx}\right)_L$ is the slope at $x = L$. At the upstream end ($x = 0$), the flow through that section will be zero. Hence the slope at that point must be

zero. Making the assumption that the slope varies linearly with x:

$$\left(\frac{dy}{dx}\right)_x = \frac{x}{L}\left(\frac{dy}{dx}\right)_L \quad \ldots\ldots (65)$$

and integrating

$$y = \left(\frac{-L^2 + x^2}{2L}\right)\left(\frac{dy}{dx}\right)_L \quad \ldots\ldots (66)$$

which is a parabola, symmetrical about the y-axis.

For one and the same slope $\left(\frac{dy}{dx}\right)_L = -\frac{q_o}{K a_o}$, the mound for stationary flow will have a greater volume than will the mound defined by Eq. 66. Therefore, there is a transition period during which the outflow remains constant. From Eq. 25 and $i = 0$ the pore volume is:

$$V_3 = \mu\left\{\left[-a_o L + \frac{K}{3 q_o}\left(a^2_o + \frac{2 q_o L}{K}\right)^{3/2} - a^3_o\right]\right\} \quad \ldots\ldots (67)$$

whereas, for the mound shape defined by Eq. 66, the pore volume

$$V_4 = \mu \frac{q_o L^2}{3 K a_o} \quad \ldots\ldots (68)$$

The change in volume is

$$\Delta V_4 = V_3 - V_4 \quad \ldots\ldots (69)$$

and since during this period the outflow is assumed to be q_o, the time is

$$\Delta T_4 = \frac{\Delta V_4}{q_o} = \frac{\mu}{q_o}\left(-a_o L + \frac{K}{3 q_o}\left[\left(a^2_o + \frac{2 q_o L}{K}\right)^{3/2} - a^3_o\right] - \frac{q_o L^2}{3 K a_o}\right) \quad \ldots (70)$$

Following this time interval the rate of outflow varies according to the unique time function:

$$q = q_o e^{-3 i l / L^2} \quad \ldots\ldots (71)$$

which satisfies the condition that its integration, with respect to t between 0 and ∞, is equal to V_4.

4.—Stationary Ground-Water Flow

The configuration of the stable mound for $i \neq 0$ was developed in Sect. 2. In the following, potential flow will be treated for $i = 0$.

Maximum Potential Flow.[11,12]—To satisfy a physically possible system of the flow net between the spreading ground and the lateral control, motion must be irrotational, and there must exist streamlines and a velocity potential, ϕ. Furthermore, the condition of continuity must be satisfied, which is expressed by the Laplace equation

$$\nabla^2 \phi = 0 \quad \ldots\ldots (72)$$

[11] "Hydraulik," by Ph. Forchheimer, B. G. Teubner, Leipzig und Berlin, 1930, pp. 82–83.

[12] "Theoretical Soil Mechanics," by Karl Terzaghi, John Wiley & Sons, Inc., New York, N. Y., 1943, pp. 239–246.

In order that this system shall represent flow under the action of gravity, the velocity potential is expressed as:

$$\phi = K\left(\frac{P}{\gamma} + y\right) \quad \ldots\ldots\ldots\ldots\ldots\ldots\ldots\ldots (73)$$

in which P = pressure and γ = unit weight of water. Along the phreatic line, P is constant or zero, so

$$\phi = K\,y \quad \ldots\ldots\ldots\ldots\ldots\ldots\ldots\ldots (74a)$$

and

$$\frac{d\phi}{dy} = K \quad \ldots\ldots\ldots\ldots\ldots\ldots\ldots\ldots (74b)$$

An analytic complex function,[13] with the added condition that $\frac{d\phi}{dy} = K$ along the phreatic line, satisfies the mathematical requirements of potential flow. To satisfy the theory strictly, the surface of the spreading ground and of the control should be at a constant potential. This condition is normally not satisfied, a situation which leads to distortions.

Changing the constants in the Kozeny[14] equation to satisfy present requirements,

$$z = \frac{1}{2\,q\,K}\,w^2 \quad \ldots\ldots\ldots\ldots\ldots\ldots\ldots\ldots (75)$$

in which:

$$z = x + iy \quad \ldots\ldots\ldots\ldots\ldots\ldots\ldots\ldots (76a)$$

and

$$w = \phi + i\psi \quad \ldots\ldots\ldots\ldots\ldots\ldots\ldots\ldots (76b)$$

in which: ϕ = a potential function; ψ = a stream function; and

$$i = \sqrt{-1}.$$

Introducing into Eq. 75 and equating real and imaginary parts,

$$x = \frac{1}{2\,q\,K}\,(\phi^2 - \psi^2) \quad \ldots\ldots\ldots\ldots\ldots\ldots\ldots\ldots (77)$$

and

$$y = \frac{1}{q\,K}\,(\phi\psi) \quad \ldots\ldots\ldots\ldots\ldots\ldots\ldots\ldots (78)$$

Constant values for ϕ and ψ determine the equipotentiality and streamlines as shown in Fig. 5. The phreatic line is defined by $\psi = q$. It is the basic parabola. The equation for the phreatic line is

$$\frac{2\,q}{K}\,x + \left(\frac{q}{K}\right)^2 = y^2 \quad \ldots\ldots\ldots\ldots\ldots\ldots\ldots\ldots (79)$$

---

[13] "Fluid Mechanics for Hydraulic Engineers," by Hunter Rouse, McGraw-Hill Book Co., Inc., New York, N. Y., 1938, pp. 96-98.

[14] "Wasserkraft und Wasserwirtschaft," by J. A. Kozeny, 1931, Vol. 26, p. 28.

Along the floor, $y = 0$, $\psi = 0$; so, from Eqs. 77 and 73:

$$\frac{P}{\gamma} = \sqrt{\frac{2\,q\,x}{K}} \quad \ldots\ldots\ldots\ldots\ldots\ldots\ldots\ldots\ldots\ldots (80)$$

which is the pressure head on the floor. Generally, $y = \frac{1}{q\,K}\,\phi\,\psi$ and $\psi = \frac{q}{n}$ in which n can be any number between 1 and ∞. Hence:

$$y = \frac{1}{q\,K}\,\frac{q}{n}\,\phi = \frac{\phi}{n\,K} \quad \ldots\ldots\ldots\ldots\ldots\ldots\ldots\ldots\ldots\ldots (81)$$

and

$$x = \frac{1}{2\,q\,K}\left(k^2\,n^2\,y^2 - \frac{q^2}{n^2}\right) \quad \ldots\ldots\ldots\ldots\ldots\ldots\ldots\ldots\ldots\ldots (82)$$

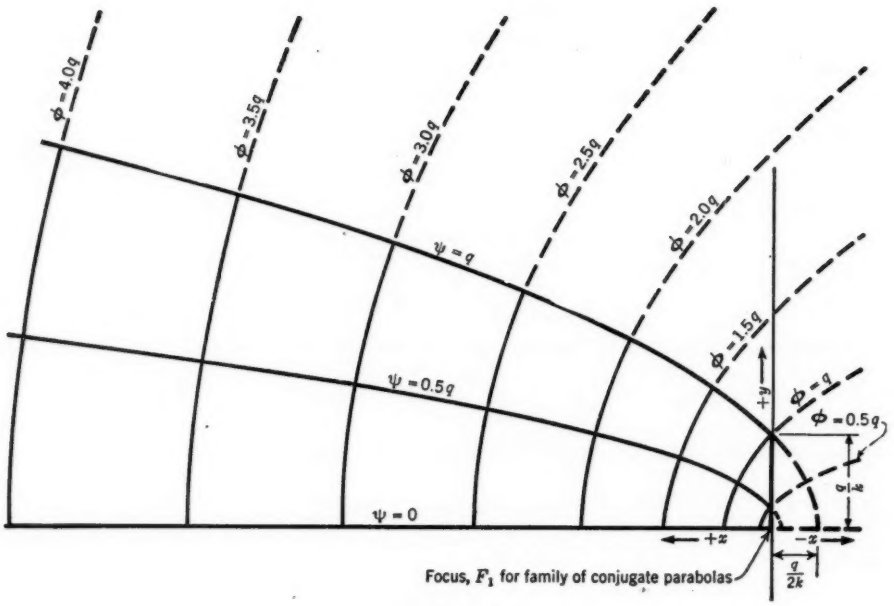

FIG. 5

Therefore, the velocity for any streamline at any point is expressed as:

$$-\,n\,K\,\frac{\partial y}{\partial s} = -\,\frac{\partial \phi}{\partial s} = v \quad \ldots\ldots\ldots\ldots\ldots\ldots\ldots\ldots\ldots\ldots (83)$$

Also, at any point on streamlines

$$\frac{dy}{dx} = \frac{q}{K\,n^2\,y} \quad \ldots\ldots\ldots\ldots\ldots\ldots\ldots\ldots\ldots\ldots (84)$$

Hence, at $x = 0$; and $y = \frac{q}{K n^2}$

$$\frac{dy}{dx} = \frac{q}{K n^2}\left(\frac{K n^2}{q}\right) = 1 \quad \ldots\ldots\ldots\ldots\ldots\ldots (85)$$

which means that at the control, the slope of every streamline is 45°. For $\frac{\partial y}{\partial s} = \sin \alpha$

$$v = -n K \sin \alpha \quad \ldots\ldots\ldots\ldots\ldots\ldots (86)$$

in which α is the angle that any streamline makes with the horizontal at any point. The horizontal transport of the streamline is—

$$v \cos \alpha = -n K \sin \alpha \cos \alpha \quad \ldots\ldots\ldots\ldots\ldots\ldots (87)$$

which is a maximum when

$$\frac{\partial}{\partial x}(v \cos \alpha) = 0 = -n K (\sin^2 \alpha - \cos^2 \alpha) \quad \ldots\ldots\ldots\ldots (88)$$

Hence, $\sin \alpha = \cos \alpha$, which is true for $\alpha = 45°$. So for the maximum discharge through the least area the slope must be 45°, which is the condition existing at $x = 0$.

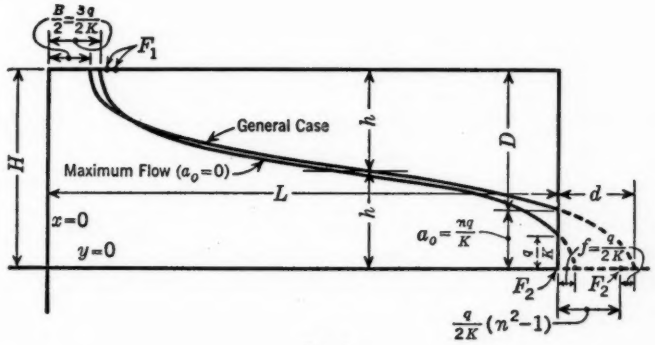

FIG. 6

This flow net represents, in general, the flow far from a spreading ground and in particular the case of a narrow spreading strip from which the water merely "rains" down upon the mound below.

The case of streamline flow from the spreading ground to the control is much more involved. Apparently no rigorous mathematical solution to the problem has so far been found. Therefore, the problem was approached as follows: As indicated in Fig. 5, the complete flow net for the basic parabola calls for the discharge q through the horizontal seepage surface between $x = 0$ and $x = -\frac{q}{2K}$. Hence, reversing and inverting the parabola, as shown in Fig. 6, results in a double parabola. If a flow q were infiltrated between F_1 and the vertex of the inverted parabola and an additional flow q were infiltrated

between the vertex and the axis of symmetry, then $\psi = q$ at the former and $\psi = 2\,q$ at the latter. From Eq. 77, $\phi = 0$ and $\psi = n\,q$; therefore

$$x = \frac{n^2\,q}{2\,K} \qquad (89)$$

Hence, the distance between $\psi = q$ and $\psi = 2\,q$ along $y = \bar{H}$ is

$$\frac{B}{2} = \frac{3}{2}\frac{q}{K} \qquad (90)$$

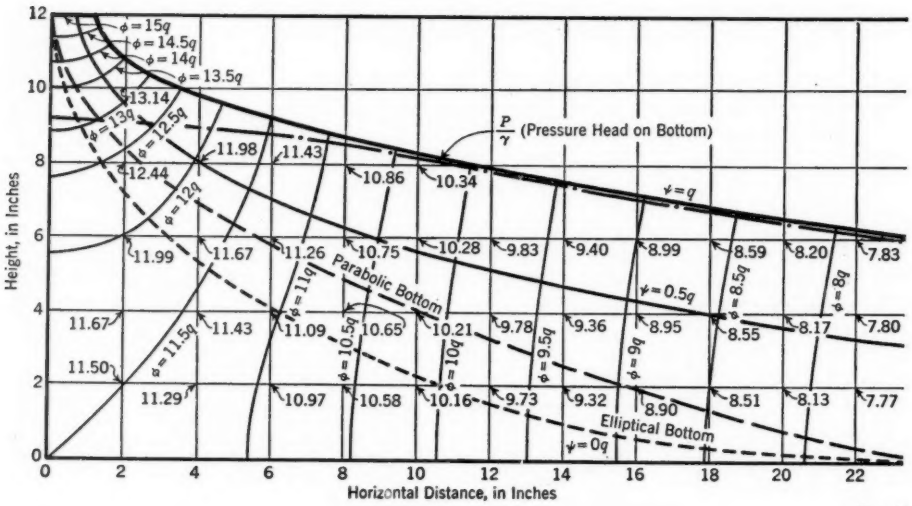

FIG. 7

and the double parabola is a streamline, common to both flow nets. Elimination of $\psi = q$ transforms this streamline into the phreatic line.

Thus far, each section of the curve has been referred to its own natural, coordinate system. The equations of the two parabolas can be referred to a common system of coordinates in which the plane of symmetry will be $x = 0$ and the impervious stratum $y = 0$ (Fig. 6).

The curve of the phreatic line between $x = \frac{3}{2}\frac{q}{K}$ and $x = \frac{L}{2} + \frac{q}{K}$ is

$$y = \bar{H} - \sqrt{\frac{2\,q\,x}{K} - \frac{3\,q^2}{K^2}} \qquad (91a)$$

and between $x = \frac{L}{2} + \frac{q}{K}$ and $x = L$:

$$y = +\sqrt{\frac{2\,q}{K}(L - x) + \frac{q^2}{K^2}} \qquad (91b)$$

Values of the equipotential ϕ will be based on the value of $\phi = 0$ at $x = L$,

$y = 0$, the point of lowest potential within the system. So, at $y = \bar{H} = 2\,\bar{h}$:

$$\phi = 2\sqrt{q\,k\,L - q^2} = \Phi' \ldots\ldots\ldots\ldots\ldots\ldots (92a)$$

At any point on the phreatic line $\phi = K\,y$ or:

$$\phi = \left(\frac{y}{\bar{H}}\right) K\,\bar{H} = \frac{y}{\bar{H}}\,\Phi' \ldots\ldots\ldots\ldots\ldots\ldots (92b)$$

The flow net between $x = 0$ and $x = \frac{L}{2} + \frac{q}{K}$ was determined by the "relaxation method,"[15] that is, by progressive approximation.

The completed flow net is shown in Fig. 7 using the following values: $L = 46$ in. $= 3.833$ ft; and $\bar{H} = 12$ in. $= 1.00$ ft. Hence from Eq. 91*a* $\frac{q}{K} = \frac{3.833 - \sqrt{3.833^2 - 1}}{2} = 0.0667$ ft. Therefore, $\frac{B}{2} = \frac{3}{2}\frac{q}{K} = 0.10$ ft $= 1.20$ in.; and $\Phi' = K\,\bar{H} = K = 15\,q$.

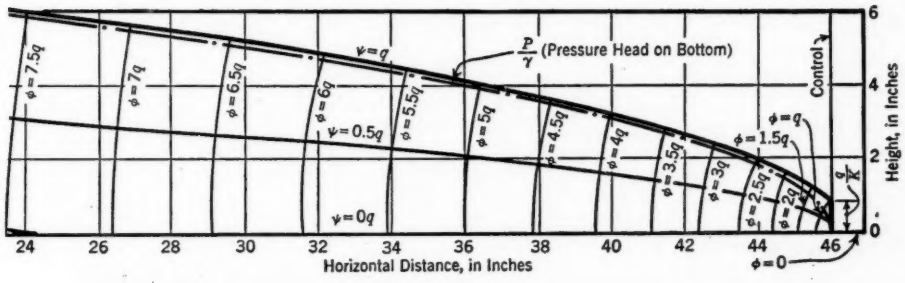

The numerical values correspond to those of the model tests on potential flow which will be discussed subsequently. The figures shown on the grid system correspond to the final approximation of the relaxation method. Partial stagnation is indicated below a boundary approximated by a quarter ellipse (Fig. 7). The parabolic boundary indicated corresponds to the one used in the model tests.

General Potential Flow.—The conditions for the general case of potential flow—that is, for any value of a_o between q/K and $\bar{H}$—are indicated in Fig. 6.

Three distinct stages of a_o must be considered, namely: (1) $0 \leqq a_o \leqq q/K$; (2) $q/K < a_o < D$; and (3) $D < a_o \leqq \bar{H}$, of which the first case has already been treated. For this case from Eq. 91*b* and from the condition that $x = L/2 + q/K$, $y = \frac{D + a_o}{2}$:

$$\frac{q}{K} = \frac{L - \sqrt{L^2 - (D + a_o)^2}}{2} \ldots\ldots\ldots\ldots\ldots\ldots (93)$$

[15] "Numerical Solutions for Tile Drainage of Layered Soils," by James N. Luthin and R. E. Gaskell, *Transactions*, American Geophysical Union, Vol. 31, 1950, p. 595.

For the second case, at downstream end:

$$y = \sqrt{\frac{2q}{K}(L + d - x)} \quad \ldots\ldots (94)$$

At $x = L$, $y = a_o$; therefore:

$$d = \frac{a^2_o K}{2q} \quad \ldots\ldots (95)$$

and

$$y = \sqrt{\frac{2q}{K}(L - x) + a^2_o} \quad \ldots\ldots (96)$$

The common point for both parabolas is at $y = \frac{D + a_o}{2}$ which lies at a distance $\frac{L + d - \frac{3q}{2K}}{2}$ from either vertex; hence at $x = \frac{L + d}{2} + \frac{3q}{4K}$, Eq. 91*a* yields:

$$\frac{q}{K} = \frac{L - \sqrt{L^2 - \frac{3}{2}(D^2 + 2Da_o - a^2_o)}}{3} \quad \ldots\ldots (97)$$

For the third case, at $x = L$, $y = a_o$ in Eq. 91*a* and

$$\frac{q}{K} = \frac{L - \sqrt{L^2 - 3D^2}}{3} \quad \ldots\ldots (98)$$

which is zero when $D = 0$.

The flow net for the downstream parabola for $q/K \leqq a_o$ still follows from Eqs. 77 and 78, the focus, however, shifting the distance—

$$x = \frac{q}{2K}(n^2 - 1) \quad \ldots\ldots (99)$$

beyond the control. At the control, along $\psi = q$:

$$y = a_o = \frac{nq}{K} \quad \ldots\ldots (100)$$

and

$$\phi = nq \quad \ldots\ldots (101)$$

Condition at the Control.—Fundamentally the problem arises because of the change in pressure along the seepage surface OA, Fig. 8, relative to that of the basic parabola. The latter pressure is shown as a cross-hatched area A_1. Under this pressure condition the flow between the equipotential surface AB and the vertical surface OA = $q_o/K = h_b$ is exactly q_o.

If the sand downstream from OA is removed, the pressure condition is changed. If $a_o = 0$, then the pressure at Sect. OA is atmospheric throughout and the pressure gradient between AB and OA is increased. Based on hori-

zontal flow paths as a simple yet fair approximation, the flow q through surface OA $\sim 1.50\ q_o$ to satisfy the Darcy law. But since the flow q_o is stationary, the seepage surface OA must adjust itself to the new pressure condition and, therefore, must reduce its height. The critical height is

$$h_c \sim \sqrt{\frac{1}{1.50}}\, h_b \sim 0.82\, \frac{q_o}{K} \qquad (102)$$

With the same degree of approximation as before it may be shown that a tailwater depth $\bar{a}_o = 0.60\ h_b$ produces pressure on Sect. OA which is similar to the pressure, represented by area A_1 in Fig. 8; that generally

$$\bar{a}_o \sim \sqrt{2\, A_1} \qquad (103)$$

and that for this condition OA $\sim q_o/K$. Finally, it is clear that for a ground-water depth $a_o > \bar{a}_o$ Sect. OA must be greater than q_o/K so that a seepage

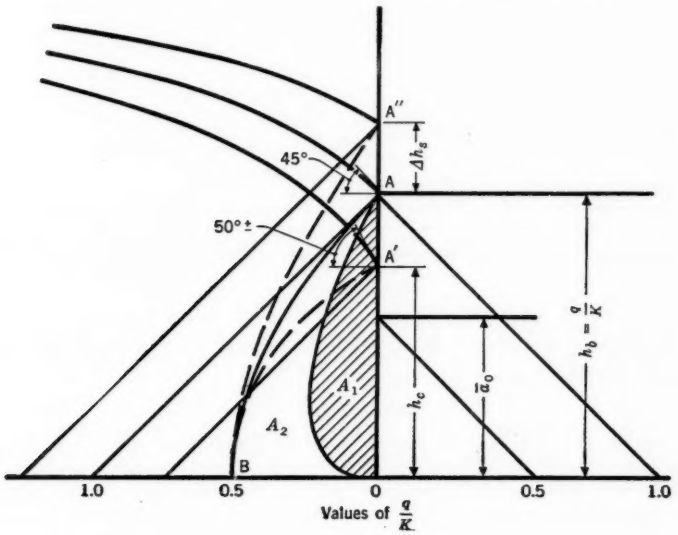

FIG. 8

surface will always maintain itself between the raised, phreatic line and the tailwater surface. For this condition the pressure gradient between A''B and OA (Fig. 8) is constant. Therefore

$$q_o \sim \frac{\Delta h_s}{\Delta L_m}\left(\frac{q_o}{K} + \Delta h_s\right) K \qquad (104)$$

in which ΔL_m = mean horizontal length of flow path which does not differ significantly from that for area ABO = A_2 of the basic parabola. Hence,

$$\Delta h_s \sim \frac{q_o}{K}\left(-\frac{1}{2} + \sqrt{\frac{1}{4} + \frac{A_2 K^2}{q^2_o}}\right) \sim 0.26\, \frac{q_o}{K} \qquad (105)$$

For $a_o > q_o/K$ the height of the seepage surface diminishes rapidly with increasing a_o and may be expressed by

$$\Delta h_s \sim 0.26 \frac{q_o}{K} \left(\frac{q_o}{a_o K} \right)^3 \ldots\ldots\ldots\ldots\ldots\ldots (106)$$

PART II.—THE THREE-DIMENSIONAL FLOW THROUGH GRANULAR SOIL

1.—Horizontal, Impervious Stratum

Circular Spreading Ground—First Phase.—If spreading is performed on an area represented by a circle, the problem must be treated as three dimensional, as shown in Fig. 9. The unsteady flow radiates uniformly from the center of the circle.

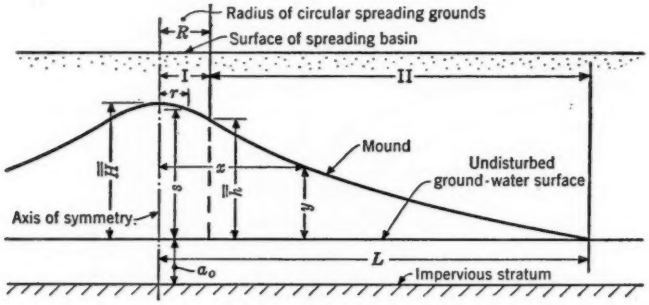

Fig. 9

Zone II.—Using a unique flow function, similar to that used for the two-dimensional mound:

$$q_o \left[1 - \frac{e\,x}{L} \left(\frac{x - R}{L - R} \right) e^{-x/L} \right] = -2\,\pi\,x\,(y + a_o)\,K \frac{dy}{dx} \ldots\ldots (107)$$

which, on integration, leads to

$$y = a_o + \sqrt{a_o^2 - \frac{q_o}{\pi K} \left[\log_e \frac{x}{L} + \frac{1}{L - R} \left((x + L - R)\, e^{(L-x)/L} - 2L + R \right) \right]} \ldots\ldots (108)$$

For $x = R$, $y = \overline{h}$; hence:

$$\overline{h} = -a_o + \sqrt{a_o^2 - \frac{q_o}{\pi K} \left[\log_e \frac{R}{L} + \frac{1}{L - R} \left((L - R)\, e^{(L-x)/L} - 2L + R \right) \right]} \ldots (109)$$

Zone I.—In Zone I, Fig. 10:

$$\Delta q\,\pi\,r^2 = -2\,\pi\,r\,(s + a_o)\,K \frac{ds}{dr} = \frac{q_o\,r^2}{R^2} \ldots\ldots\ldots\ldots (110)$$

in which Δq is the spreading rate per unit area. Integrating:

$$s = -a_o + \sqrt{(\overline{H} + a_o)^2 - \frac{q_o r^2}{2\pi K R^2}} \quad \ldots\ldots\ldots\ldots (111)$$

For $r = R$, $s = \overline{h}$ and, therefore, from Eqs. 109 and 111:

$$\overline{H} = -a_o + \sqrt{a_o^2 - \frac{q_o}{\pi K}\left[\log_e \frac{R}{L} + \frac{1}{L-R}\left((L-R)\,e^{(L-R)/L} - 2L + R\right) - \frac{1}{2}\right]} \quad (112)$$

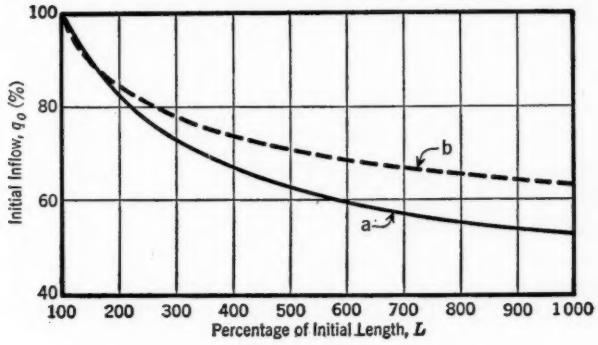

FIG. 10

For zone II and for $a_o \gg \overline{H}$ the binomial expansion of Eq. 108 may be used as an approximation. Thus

$$y = -\frac{q_o}{2K a_o}\left[\log_e \frac{x}{L} + \frac{1}{L-R}\left((x + L - R)\,e^{(L-x)/L} - 2L + R\right)\right] \ldots (113)$$

and the volume of water stored in the pores is

$$V''' = \frac{\mu q_o}{K a_o}\left[\frac{L^2}{4} + \frac{8L^3 - \frac{5L^2R}{2} - LR^2 + \frac{R^3}{2}}{L-R} - \frac{e^{(L-R)/L}}{L-R}(3L^3 + 2RL^2) + \frac{R^2}{2}\left(\log_e \frac{R}{L} - \frac{1}{2}\right)\right] \ldots (114)$$

Recharge Well—First Phase.—If, instead of a circular spreading ground, a well is used in recharge of ground water, then R relative to L, and the storage in the well, may be neglected. Then approximately:

$$V''' = \frac{\mu q_o}{10 K a_o} L^2 = q_o T''' \ldots\ldots\ldots\ldots (115)$$

in which T''' = total spreading time. Hence:

$$T''' = \frac{\mu}{10 K a_o} L^2 \ldots\ldots\ldots\ldots (116)$$

Circular Spreading Ground—Second Phase.—It would not be reasonable to consider the analogue of case (a) as previously analyzed, in connection with the three-dimensional mound because of the improbability of the existence of a circular control. However, the analogue of case (b) is all the more important.

When the three-dimensional mound has risen to the potential control, it follows from Eq. 109 that for $\bar{\bar{h}}$ to remain constant L and q_o must be related at all times as shown in Fig. 10, curve a. It is based on typical numerical values, namely, $R = 500$ and initial length $L = 5{,}000$ ft.

Recharge Well—Second Phase.—As R is small as compared to L, the second term under the radical in Eq. 109 reduces to $\frac{q_o}{\pi K}(\log_e R/L + 0.72)$ which for a typical, initial ratio $R/L = 0.01$ leads to the relation shown in Fig. 10 as curve b.

2.—Inclined, Impervious Stratum

It is possible to gain an insight into this complex case by assuming[16] the spreading flow as originating from a source of strength m, discharging vertically onto an inclined plane of infinite width and length. If the source is assumed at the origin and if U = initial uniform ground-water flow per linear ft, parallel to the x-axis, then:

$$U = K a_o i \ldots\ldots\ldots\ldots\ldots\ldots\ldots\ldots (117a)$$

and if

$$2\pi m = q_o \ldots\ldots\ldots\ldots\ldots\ldots\ldots\ldots (117b)$$

then the combined flow of the initial uniform flow, U, and the spreading flow q_o, can be represented by the complex function:

$$w = -Uz - m\log_e z \ldots\ldots\ldots\ldots\ldots\ldots\ldots (118)$$

In view of the definition of w and z, previously shown

$$\phi = -Ux - m\log_e (x^2 + y^2)^{\frac{1}{2}} \ldots\ldots\ldots\ldots\ldots\ldots (119)$$

and

$$\psi = -Uy - m\tan^{-1} y/x \ldots\ldots\ldots\ldots\ldots\ldots\ldots (120)$$

The flow net based on these equations may be drawn by Rankin's graphical method[17] and is shown in Fig. 11. The boundary of the mound is given by the streamline $\psi = 0$; so, from Eq. 119

$$y = -x\tan\frac{Uy}{m} \ldots\ldots\ldots\ldots\ldots\ldots\ldots\ldots (121)$$

from which it follows that the boundary asymptotically approaches—

$$y = \pm\frac{m}{U} = \pm h_o \ldots\ldots\ldots\ldots\ldots\ldots\ldots\ldots (122)$$

---

[16] "Theoretical Hydrodynamics," by L. M. Milne-Thomson, Macmillan Co., Inc., New York, N. Y., 1950.

[17] "Elementary Demonstrations of Principles Relating to Stream-lines," by W. J. Macquorn Rankine, *Miscellaneous Scientific Papers*, Charles Griffin and Co., London, 1881, p. 522.

as $x \rightarrow \infty$ and that the mound extends upstream to the stagnation point

$$x_o = -\frac{h_o}{\pi} \quad \ldots\ldots\ldots\ldots\ldots\ldots\ldots\ldots\ldots\ldots (123)$$

Substituting for U and m in Eq. 122 gives the mound width at $x = \infty$:

$$W = 2\,h_o = \frac{q_o}{K\,a_o\,i} \quad \ldots\ldots\ldots\ldots\ldots\ldots\ldots\ldots\ldots\ldots (124)$$

Thus, the mound boundary has the effect of a training wall and relative to the initial ground-water stream of infinite width, the mound acts like an island of finite width and semi-infinite length.

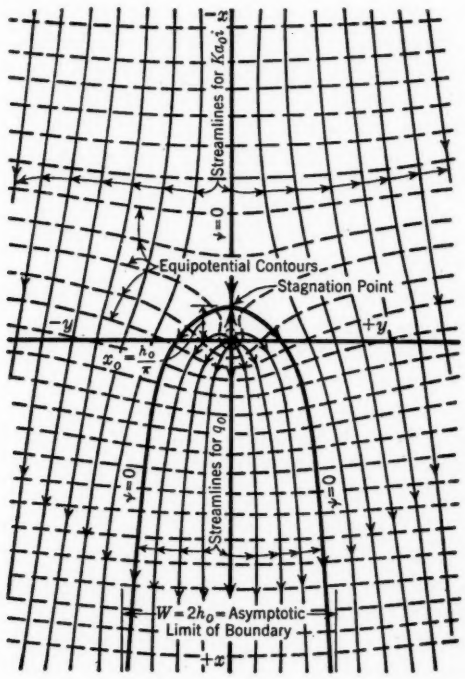

FIG. 11

Numerical Evaluation of Equations.—The following quantities are typical for one of the existing spreading grounds, the area of which may be approximated by that of a relatively small circle, namely: $R = 500$ ft; $a_o = 100$ ft; $K = 100$ ft per hr; and $q_o = 1 \times 10^6$ ft^3 per hr. Hence for $i = 0.01$ from Eq. 124, $W = \frac{q_o}{K\,a_o\,i} = 10{,}000$ ft; and from Eq. 123 $x_o = -\frac{5{,}000}{\pi} = -1{,}592$ ft. In this case, based on the potential function the rise of the mound above the normal ground-water surface is of the order of 35 ft. This is its ultimate height.

For $i = 0$ and $L = 5{,}000$ ft, from Eq. 112, $\overline{\overline{H}} = 33.47$ ft and from Eq. 114 $V''' = 34.23 \times 10^6$ ft^3 = 786 acre ft and $T''' = 34.23$ hr of spreading.

This clearly brings out the magnitude of the mound for $i = 0$ even during short spreading operations. They often extend over much longer periods.

PART III.—THE MODEL TESTS ON TWO-DIMENSIONAL GROUND-WATER FLOW

1.—Description of the Model Setup

Two distinct model arrangements were used to test the mechanics of the four phases for two-dimensional flow. The model sand was clean, hard, stream-worn material which had passed a no. 30 screen and had been retained on a no. 40 screen. The grain size, therefore, varied little from 0.5 mm.

First Model Arrangement.—The first model arrangement served to ascertain the wave phenomenon and unsteady flow characteristics during the first and second phases, the outflow hydrograph during the second phase, and the drainage of the mound during the fourth phase. A general view of the model setup in connection with this arrangement is shown in Fig. 12, and details of the model proper are shown in Fig. 13. The latter consisted of:

a. A watertight box approximately 12 in. wide, 12 in. deep, and 46 in. long, filled with sand with a grid-lined glass front;

b. A metal frame, 4 in. wide at the upstream end, simulating the spreading ground and extending clear across the box;

c. Twenty-five piezometers arranged in horizontal sets of five, each at five elevations above the bottom and each set extending 2 in., 4 in., 6 in., 8 in., and 10 in., respectively, into the sand from the end wall;

d. Eight deep wells, each equipped with threaded brass rod and steel contact point, adjustable as to vertical position within 0.005 in., and connected to a direct-current low voltage source;

e. Nine shallow wells behind and parallel to the deep wells, and equipped with one movable contact point of the same design as previously described;

f. Nine argon bulbs to indicate visually the instant of contact between the ground-water surface and the point gages;

g. A lateral control comprising a 40-mesh vertical screen, a tail bucket, and an adjustable weir for the control of the initial and final ground-water depths as well as for a check on the outflow;

h. An automatic chronograph, comprising nine active supersensitive relays and one spare supersensitive relay equipped with arms and pens for recording of the aforementioned well-point contacts in terms of time (the latter being controlled by a separate clock, recording 1-sec time intervals);

i. An automatic stage recorder to ascertain rate of outflow in terms of time;

j. A constant-head tank with float valve control, fed from a large primary tank and connected to a municipal source of water supply; and

k. An orifice-equipped manometer to determine the rate of inflow to the model. The rate of inflow was controlled by a needle valve, and the water

was delivered to the spreading ground by a swing spout. The latter served to take volumetric measurements when desired.

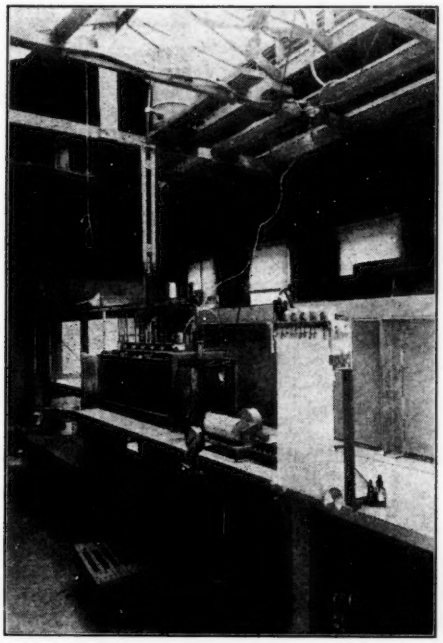

FIG. 12

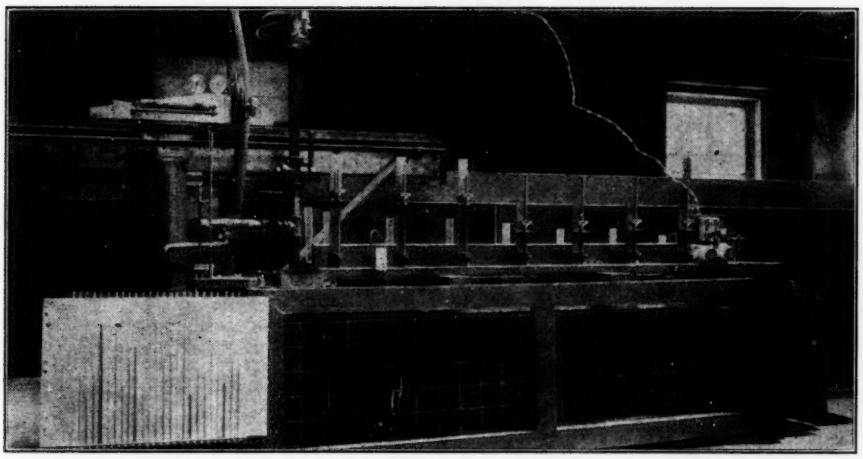

FIG. 13

Minimum aeration and uniform distribution of inflow into the spreading ground were accomplished by a trough, connected to a manifold with twenty-four small spouts placed at the surface of a ½-in. layer of coarse diffuser sand

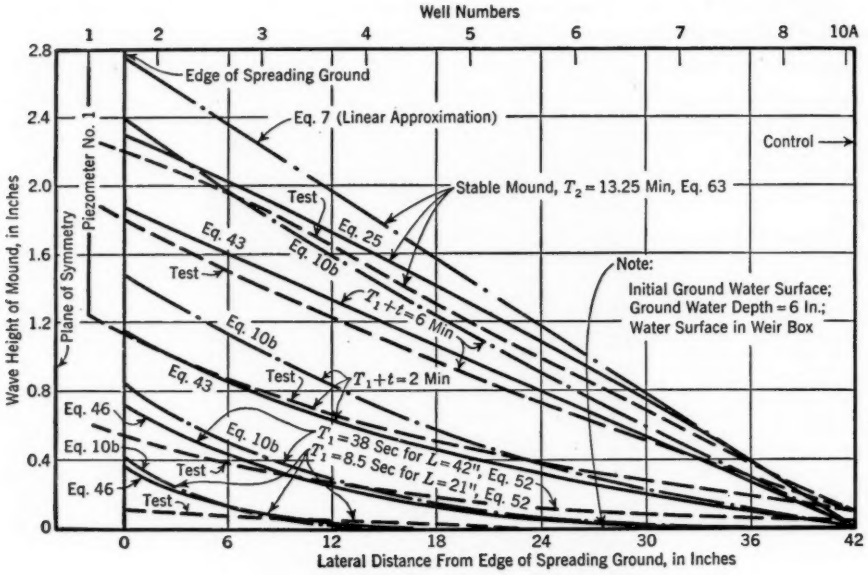
Well Numbers
1
2
3
4
5
6
7
8
10A
Edge of Spreading Ground
Eq. 7 (Linear Approximation)
Control
Stable Mound, $T_2 = 13.25$ Min, Eq. 63
Test
Eq. 25
Eq. 43
Eq. 10b
Test
Note:
Initial Ground Water Surface;
Ground Water Depth = 6 In.;
Water Surface in Weir Box
$T_1+t=6$ Min
Eq. 10b
Eq. 43
Test
$T_1+t=2$ Min
Eq. 46
Eq. 10b
$T_1=38$ Sec for $L=42$", Eq. 52
$T_1=8.5$ Sec for $L=21$", Eq. 52
Test
Eq. 46
Test
Wave Height of Mound, in Inches
Plane of Symmetry
Piezometer No. 1
2.8
2.4
2.0
1.6
1.2
0.8
0.4
0
0
6
12
18
24
30
36
42
Lateral Distance From Edge of Spreading Ground, in Inches

FIG. 14

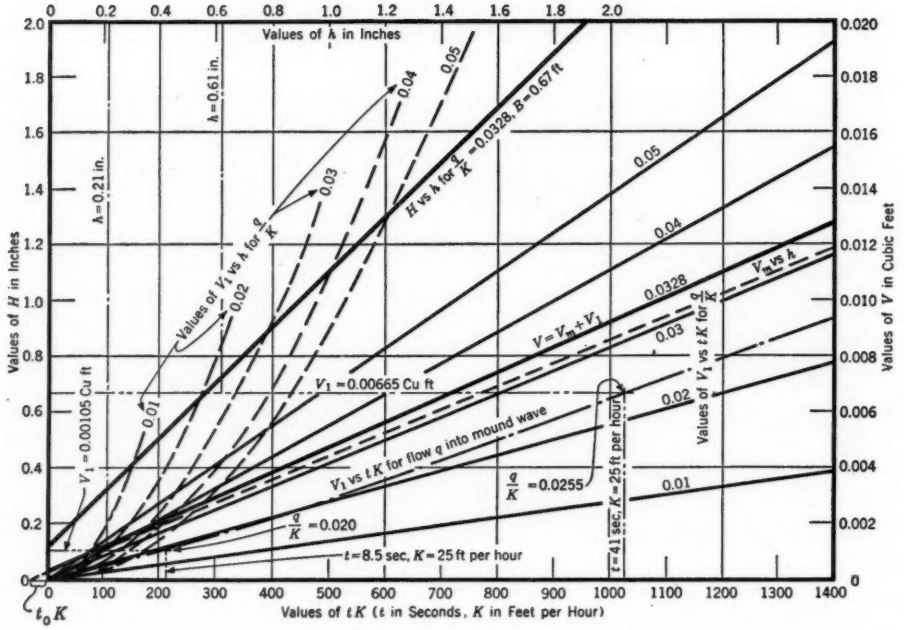
Values of h in Inches
$h=0.61$ in.
$h=0.21$ in.
0.04
0.05
H vs h for $\frac{q}{K}=0.0328$, $B=0.67$ ft
0.05
0.04
0.0328
0.03
0.02
0.01
Values of V_1 vs h for $\frac{q}{K}$
$V=V_2+V_1$
V_2 vs t
Values of V_1 vs tK for $\frac{q}{K}$
$V_1=0.00665$ Cu ft
$V_1=0.00105$ Cu ft
V_1 vs tK for flow q into mound wave
$\frac{q}{K}=0.0255$
$\frac{q}{K}=0.020$
$t=41$ sec, $K=25$ ft per hour
$t=8.5$ sec, $K=25$ ft per hour
Values of H in Inches
Values of V in Cubic Feet
t_0K
Values of tK (t in Seconds, K in Feet per Hour)

FIG. 15

overlying the test sand. A small U-tube connected to the bottom of the spreading-ground frame served to detect air lock, if present.

Second Model Arrangement.—The second model arrangement served to ascertain the validity of the theory on potential flow. For this purpose both deep and shallow wells were removed, together with the electrical recording apparatus and the water-stage recorder at the discharge end.

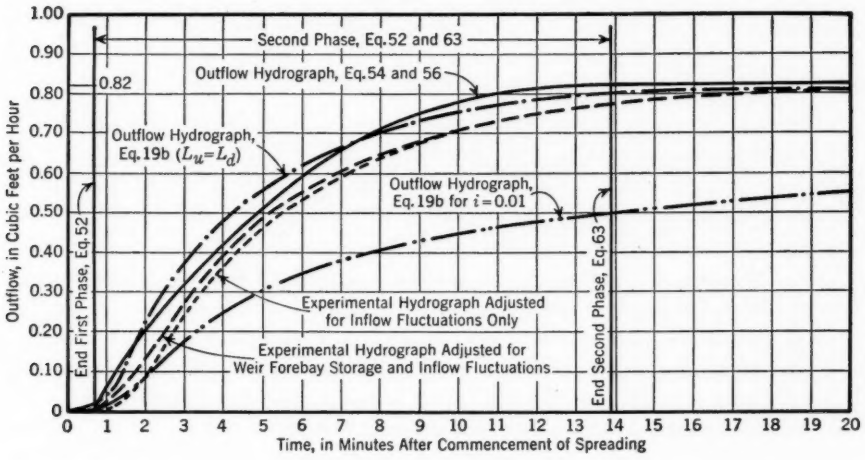
Second Phase, Eq.52 and 63
Outflow Hydrograph, Eq.54 and 56
0.82
Outflow Hydrograph, Eq.19b ($L_u=L_d$)
Outflow Hydrograph, Eq.19b for $i=0.01$
End First Phase, Eq.52
End Second Phase, Eq.63
Experimental Hydrograph Adjusted for Inflow Fluctuations Only
Experimental Hydrograph Adjusted for Weir Forebay Storage and Inflow Fluctuations
Outflow, in Cubic Feet per Hour
Time, in Minutes After Commencement of Spreading

FIG. 16

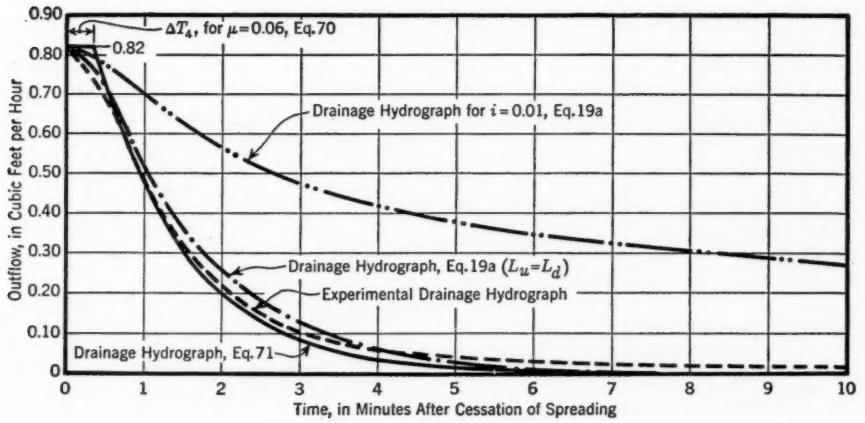
ΔT_4, for $\mu=0.06$, Eq.70
0.82
Drainage Hydrograph for $i=0.01$, Eq.19a
Drainage Hydrograph, Eq.19a ($L_u=L_d$)
Experimental Drainage Hydrograph
Drainage Hydrograph, Eq.71
Outflow, in Cubic Feet per Hour
Time, in Minutes After Cessation of Spreading

FIG. 17

The depth of the sand was increased to 12 in., the length kept at 46 in., and the spreading ground was reduced to 1.20 in. in width, in line with the dimensions used in the theoretical study (Fig. 7); eight piezometers were added to the original twenty-five in the end wall, and thirty-nine piezometers were installed in the back wall, as shown subsequently in Fig. 18. They extended 2 in. into the sand.

Next, the sand was removed from the surface down to within 0.5 in. of the theoretical phreatic line in accordance with Fig. 7, except near the spreading ground where a small wedge of sand was left for stability.

Finally all the sand was removed. A parabolic boundary was constructed with the focus of the phreatic line and the vertical end wall as a tangent and with a transition to the horizontal floor near the midpoint. The sand was replaced to 0.5 in. over the theoretical phreatic line to conform to the previous condition.

2.—The Model Test Runs

All four phases of the mound phenomenon were included in the model tests. The rates of flow, actually observed in the model (which has the neat width of 11.25 in.) are distinguished from the rate of flow per linear foot, by Q. Rates of flow corrected for a width of 12 in. are shown by q. The latter are based, therefore, on the same premise as the theoretical rates of flow.

For the purpose of recording the first and second phases by the chronograph, the point gages in the wells were connected to the positive pole, and the ground water was connected to the negative pole of a direct-current circuit.

A comprehensive test of the first two phases was conducted for a ground-water stage $a_o = 6$ in., consisting of many consecutive runs at constant $q_o = 0.82$ cu ft per hr. During this time all the eight contact points were set at progressively higher levels to obtain the configuration of the unstable mound above the undisturbed ground-water surface in terms of time.

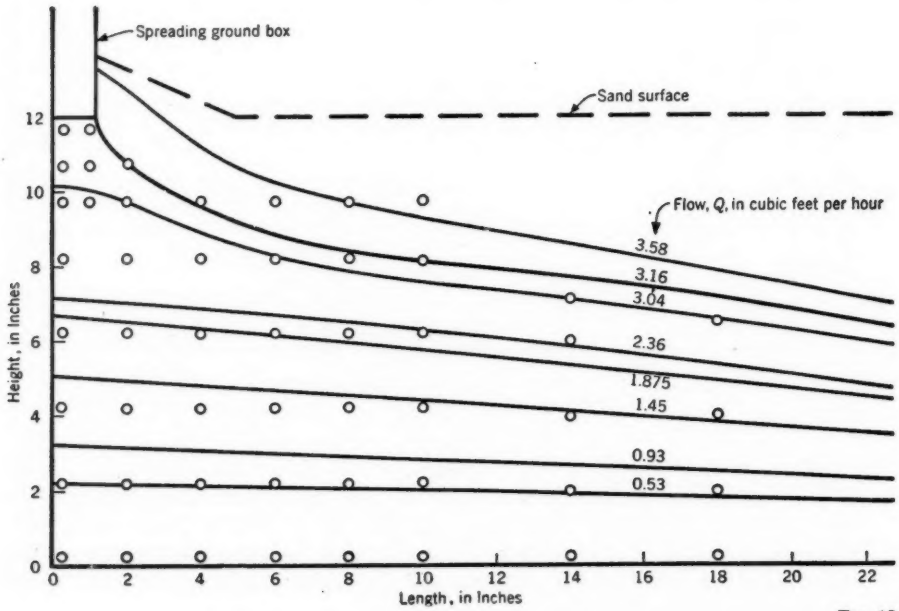

Fig. 18

The stationary flow of the third phase was investigated by test runs on various initial ground-water stages a_o with the prime objective of establishing q_o (max) for each stage under this condition. It was not possible to maintain a continuous pressure system between the spreading ground ($B/2 = 4.00$ in.) and the control.

Tests for the fourth phase immediately followed those for the third phase. The rate of drainage was recorded automatically by the water-stage recorder. The recordings were supplemented by direct, volumetric measurements.

After rearranging the model as previously outlined, the test runs on potential flow were conducted:

1. With the sand surface 12 in. above the bottom;
2. With the sand surface shaved down to within 0.5 in. of the theoretical phreatic line as shown in Fig. 7; and
3. With the sand surface the same as in condition 2 and in addition with a parabolic lower boundary between $x = 0$ and $x \sim L/2$.

Fluorescein was injected into the spreading basin, and at intervals of 1 min, 2 min, or 5 min the progress of this fluorescein was traced on the glass that formed the face of the model, giving what may be called "travel fringes." In addition, dye was inserted adjacent to the glass at various elevations of the test length, and streamlines were drawn from the movement of this dye. Under this condition there was no difficulty in maintaining a continuous pressure system between the spreading ground ($B/2 = 1.20$ in.) and the control.

3.—Comparison Between Theory and Test Results

Comprehensive Tests.—Numerical values corresponding to the model tests were introduced into the equations. Since the floor of the model was horizontal, only those equations based on $i = 0$ were considered, except for the outflow from the mound during its growth and disappearance which was also computed for $i = 0.01$ for the sake of comparison.

The Reynolds number for the test sand, based on a unit gradient and a water temperature of 60° F, was 0.4. Hence, the flow was well within the

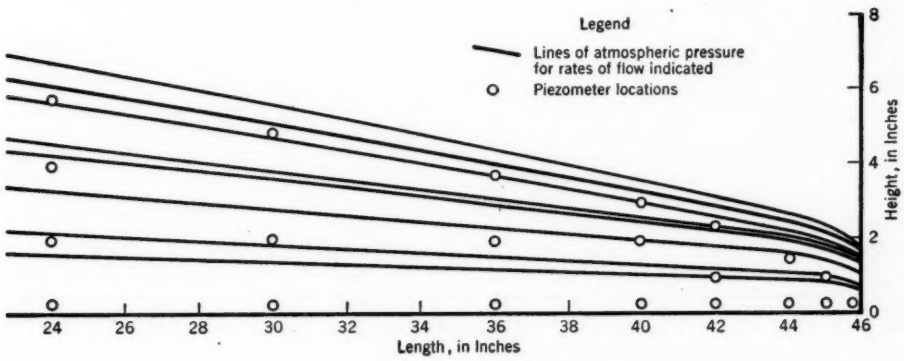

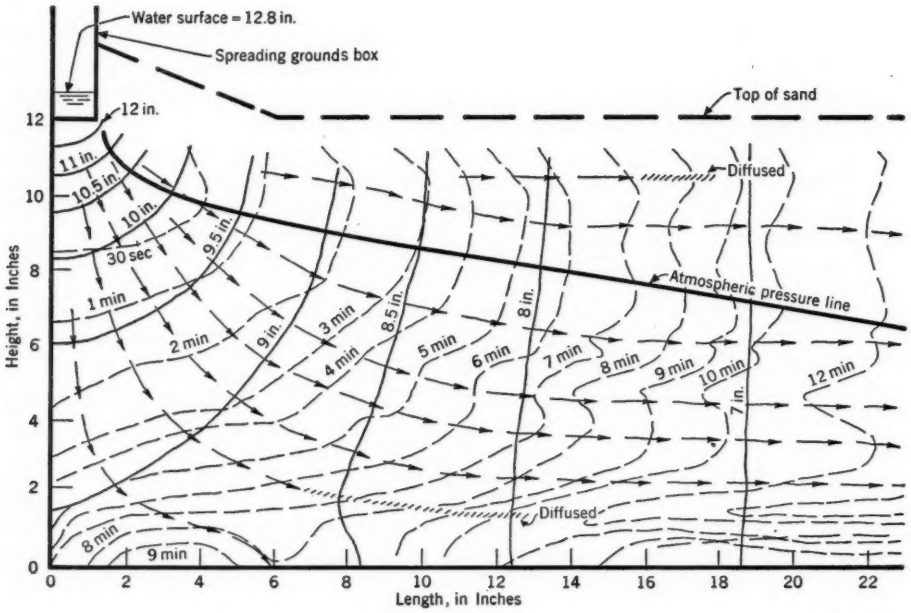
Water surface = 12.8 in.
Spreading grounds box
Top of sand
12 in.
11 in.
10.5 in.
10 in.
9.5 in.
30 sec
1 min
2 min
9 in.
3 min
4 min
8.5 in.
5 min
8 in.
6 min
7 min
8 min
9 min
10 min
12 min
7 in.
Diffused
Atmospheric pressure line
Diffused
8 min
9 min
Height, in Inches
Length, in Inches
0
2
4
6
8
10
12
14
16
18
20
22

FIG. 19

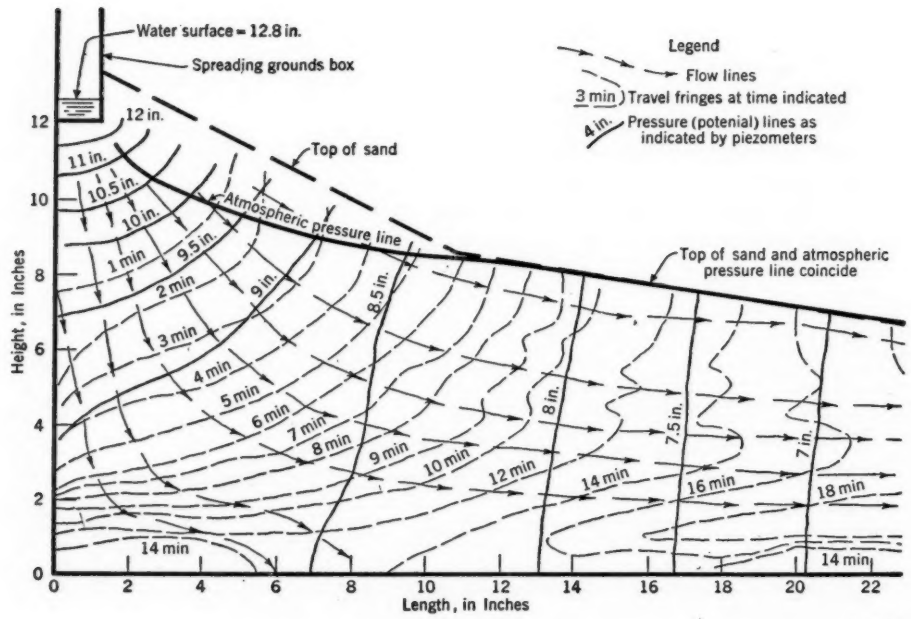
Water surface = 12.8 in.
Spreading grounds box
Legend
Flow lines
3 min Travel fringes at time indicated
4 in. Pressure (potenial) lines as indicated by piezometers
12 in.
Top of sand
11 in.
10.5 in.
Atmospheric pressure line
10 in.
9.5 in.
1 min
2 min
9 in.
3 min
8.5 in.
4 min
5 min
6 min
7 min
8 min
9 min
10 min
12 min
14 min
8 in.
7.5 in.
16 min
18 min
7 in.
Top of sand and atmospheric pressure line coincide
14 min
Height, in Inches
Length, in Inches
0
2
4
6
8
10
12
14
16
18
20
22

FIG. 20

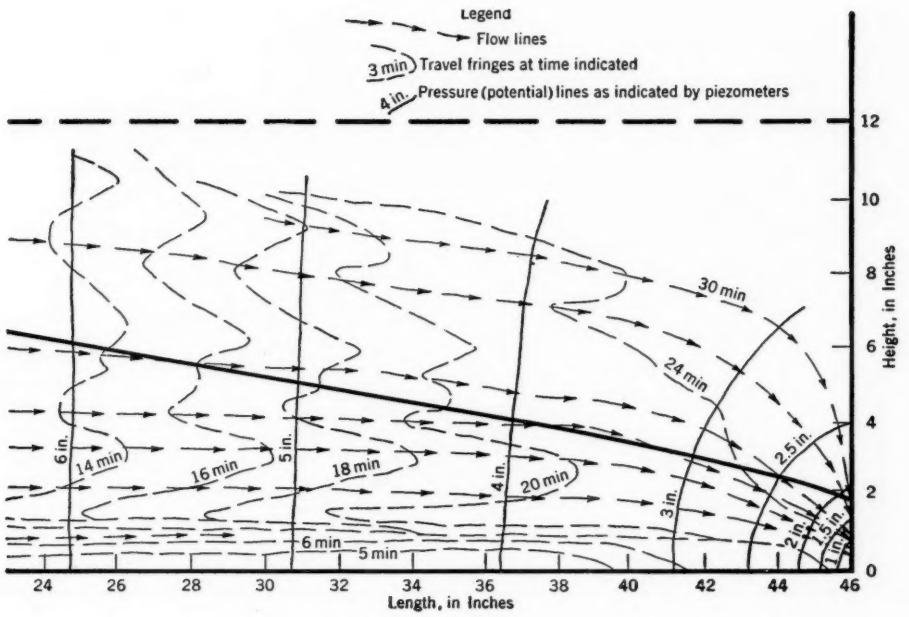

laminar range. The permeability coefficient K of the model sand averaged 25 ft per hr at 60° F. A value of $\mu = 0.15$ represents average conditions of porosity for the rising stage; and $\mu = 0.06$ represents average conditions of porosity for the falling stage within the range of the mound of the comprehensive tests.

Figs. 14 to 17 show the evaluation of Eqs. 7, 10*b*, 19, 25, 43, 44, 46, 47, 52, 55, 56, 63, 70, and 71 pertaining to all the four phases. Numerical values used were $a_o = 0.5$ ft; $q_o = 0.82$ cu ft per hr per unit width; $K = 25$; and μ equals a value between 0.15 and 0.06. The rate of propagation of the wave front during the first phase was governed by a contact-point setting of 0.005 in.

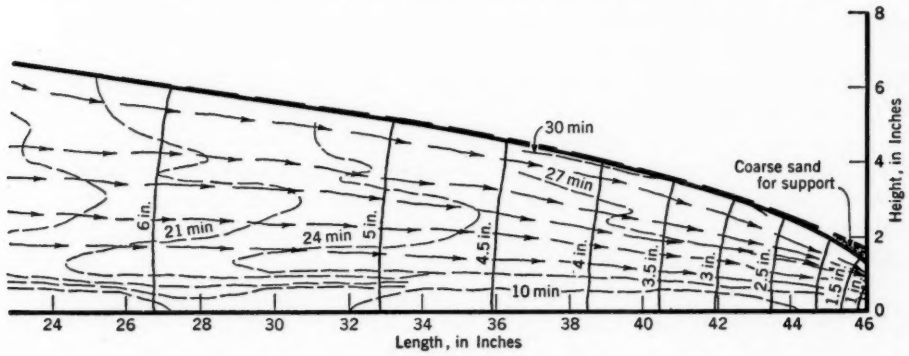

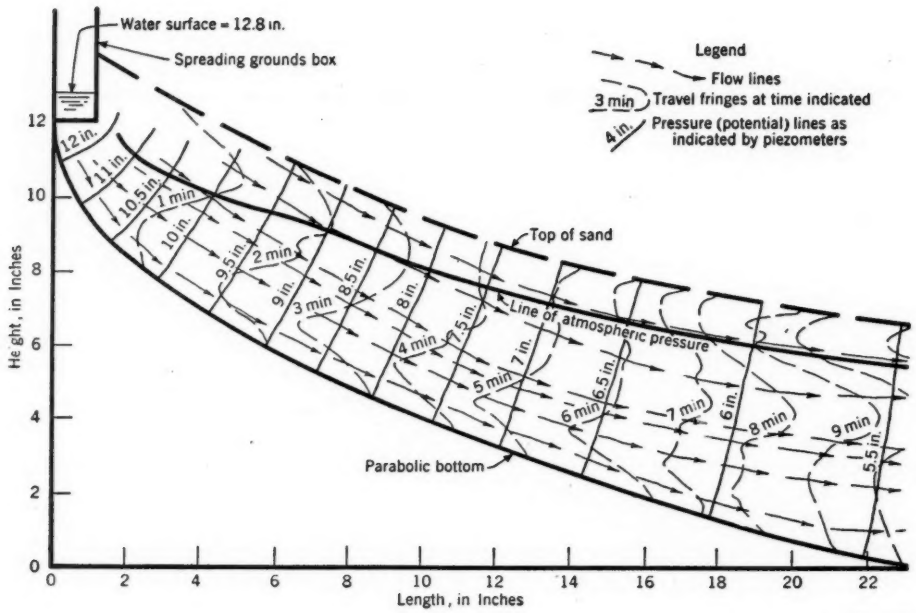

FIG. 21

above the initial ground-water surface. The observed average rate over the length of the model was approximately 330 ft per hr. It is closely checked by the theoretical rate (Fig. 14). Based on $K = 25$ ft per hr and an average slope of 0.015, the corresponding average velocity of steady flow would be 0.375 ft per hr or nearly one nine hundredth of the average wave velocity. This explains the surprisingly short time intervals, often observed in the field, between beginning of spreading operations and the rise of the water surface in remote observation wells.

As previously stated, the effect of storage ΔV_m in the mound directly beneath the spreading ground was neglected in the derivation of the equations for the unsteady mound wave. Therefore, the respective correction was accomplished graphically as shown in Fig. 15. For the observed ratio $q_o/K = 0.0328$ and $\mu = 0.15$ this correction of the theoretical wave height h eliminates the major part of the discrepancy between experimental and theoretical values. Since the flow into the mound wave was affected by capillarity in addition to the storage ΔV_m, a flat check could not be expected. Both influences diminish with an increase in h and, therefore, with V_1. In a strict sense, Fig. 15 is applicable only to the first phase.

Potential Flow Tests.—Fig. 18 shows the test result for various rates of observed stationary flow Q for condition (1), which was necessarily affected by capillary flow. Hence the rates of flow shown at corresponding atmospheric pressure lines included the latter.

Fig. 19 shows the result for condition 1 for $q = 3.52$ ft per hr, $K = 24$ ft per hr, and $\bar{H} = 12.80$ in. Streamlines, equipotential lines, and travel fringes are indicated. Flow through the entire prism, except near the control, is evident. Fig. 20 shows the result for condition 2 for $q = 2.20$ cu ft per hr and $K = 22.6$ ft per hr. Hence, $q/K = 0.097$ ft² as compared to 0.067 ft², the dimension per linear foot being understood in this discussion of the tests for $\bar{H} = 12$ in. on which Fig. 7 is based. Capillary flow is evident in the small wedge of sand next to the spreading ground which could not be removed for reasons of stability. Partial stagnation in the lower left-hand corner is con-

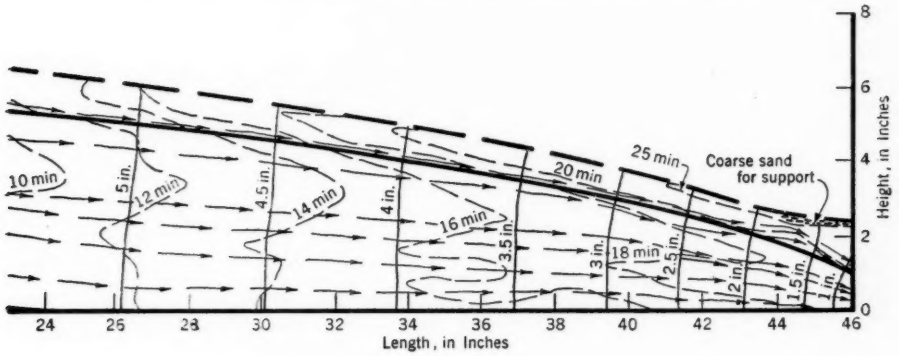

spicuous, and so is the concentration of flow immediately below the phreatic line in the upstream half of the model. The effective head $\bar{H}$ averaged 12.80 in. and, therefore, was in excess of the theoretical one as shown in Fig. 7. The extra head was necessary to assure positive pressure on the floor of the spreading ground. The phreatic line maintained itself above the theoretical one as would be expected, except within the aforementioned wedge. Removal of even the smallest amount of sand from the parabolic surface below the wedge caused free water to appear. There was no difficulty in maintaining reasonably constant q and $\bar{H}$.

Fig. 21 shows the result for condition 3. Replacing the sand after installation of the parabolic floor resulted in a permeability which was greater than in the preceding test—namely $K = 24$ ft per hr. Hence, for the corrected observed $q = 1.95$ ft³ per hr q/K was 0.081 ft². It is interesting to note that the phreatic line, contrary to the preceding test, dropped below the surface of the sand where it remained parallel to the surface. Therefore, the parabolic boundary tended to give rise to a similar rate of flow as for condition 2 through smaller cross sections. Although tests for an elliptical, lower boundary as indicated in Fig. 7 were not conducted, it appears logical to presume that the agreement in q, between this case and condition 2, would have been closer yet than for the parabolic boundary.

In general, the results obtained from the model tests, if proper allowance for capillarity is made, fall close to the theoretical ones and, therefore, may be considered a satisfactory verification of the theory of the mound phenomenon.

Acknowledgment

The writer is indebted to H. E. Hedger, M. ASCE, chief engineer of the Los Angeles County Flood Control District, for reviewing the paper and offering practical suggestions; to Maxwell F. Burke, Assoc. M. ASCE, who supervised the model tests; to Karl F. Smallin and Milan W. Ransom, Assoc. M. ASCE, whose mechanical skill and perseverance were instrumental in the achievement of the comprehensive test results; and to Richard W. Rutowski for conducting the tests on potential flow, for checking the mathematical work, and for his assistance and initiative in the evaluation of equations.

AMERICAN SOCIETY OF CIVIL ENGINEERS

OFFICERS FOR 1951

PRESIDENT

GAIL A. HATHAWAY

VICE-PRESIDENTS

Term expires January, 1952:

FRED C. SCOBEY
ALBERT HAERTLEIN

Term expires October, 1952:

WILLIAM R. GLIDDEN
DANIEL V. TERRELL

DIRECTORS

Term expires January, 1952:

WALDO G. BOWMAN
HAROLD L. BLAKESLEE
PAUL L. HOLLAND
EDMUND FRIEDMAN
S. T. HARDING

Term expires January, 1953:

OTTO HOLDEN
FRANK L. WEAVER
GORDON H. BUTLER
G. BROOKS EARNEST
WALTER J. RYAN
GEORGE W. LAMB

Term expires October, 1952:

MORRIS GOODKIND
MILTON T. WILSON

Term expires October, 1953:

KIRBY SMITH
FRANCIS S. FRIEL
LOUIS R. HOWSON
WALLACE L. CHADWICK
NORMAN R. MOORE
BURTON G. DWYRE

PAST-PRESIDENTS

Members of the Board

FRANKLIN THOMAS
ERNEST E. HOWARD

TREASURER

CHARLES E. TROUT

EXECUTIVE SECRETARY

WILLIAM N. CAREY

ASSISTANT TREASURER

GEORGE W. BURPEE

ASSISTANT SECRETARY

E. L. CHANDLER

PROCEEDINGS OF THE SOCIETY

SYDNEY WILMOT
Manager of Technical Publications

HAROLD T. LARSEN
Editor of Technical Publications

JOHN C. REHFIELD
Assoc. Editor of Technical Publications

COMMITTEE ON PUBLICATIONS

WALDO G. BOWMAN

FRANCIS S. FRIEL
S. T. HARDING
OTTO HOLDEN
LOUIS R. HOWSON
NORMAN R. MOORE